PART IIA

pn JUNCTION DIODES

5 *pn* Junction Electrostatics

In Part II we primarily examine devices whose operation is intimately tied to the one or more *pn* junctions built into the structure. Considerable attention is initially given to the charter member of the device family, the *pn* junction diode. The diode analysis in Part IIA is of particular importance because it establishes basic concepts and analytical procedures that are of universal utility. Special *pn* junction diodes are described at the end of Part IIA in the "read-only" chapter on optoelectronic diodes. In Part IIB the concepts and procedures are applied and somewhat expanded in treating another important member of the family, the two-junction, three-terminal, bipolar junction transistor (BJT). Devices with more than two *pn* junctions are briefly considered in the chapter on PNPN devices. The concluding chapter in Part IIB treats metal–semiconductor contacts and the Schottky diode, a "cousin" of the *pn* junction diode.

A complete, systematic device analysis is typically divided into four major segments. Providing the foundation for the entire analysis, the first treats the charge density, the electric field, and the electrostatic potential—collectively referred to as the electrostatics—existing inside the device under equilibrium and steady state conditions. Subsequent segments are in turn devoted to modeling the steady state (d.c.) response, the small-signal (a.c.) response, and the transient (pulsed) response of the device. The *pn* junction diode analysis to be presented follows the noted four-step development. In this chapter we take the first step by exploring the electrostatics associated with a *pn* junction.

5.1 PRELIMINARIES

5.1.1 Junction Terminology/Idealized Profiles

Suppose for the sake of discussion that a *pn* junction has been formed by diffusing a *p*-type dopant into a uniformly doped *n*-type wafer. The assumed situation is pictured in Fig. 5.1(a). In the near-surface region where the in-diffused $N_A > N_D$, the semiconductor is obviously *p*-type. Deeper in the semiconductor where $N_D > N_A$, the semiconductor is *n*-type. Clearly, the dividing line between the two regions, known formally as the *metallurgical junction,* occurs at the plane in the semiconductor where $N_D - N_A = 0$.

Note that only the *net* doping is relevant in determining the position of the metallurgical junction. Only the net doping concentration is likewise required in establishing the electrostatic variables. Thus, instead of presenting superimposed plots of N_A and N_D versus x as in Fig. 5.1(a), it is more useful to combine N_A and N_D information into a single

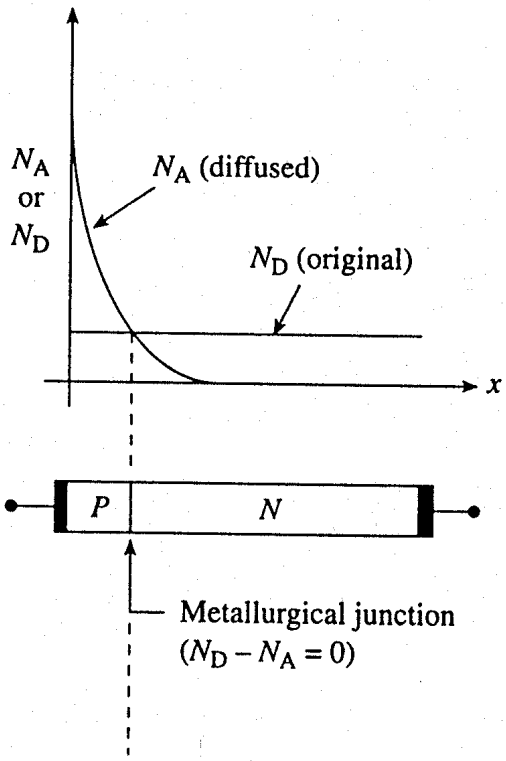

(a)

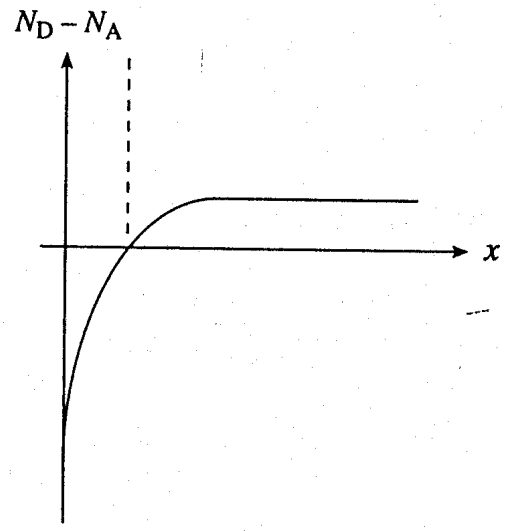

(b)

Figure 5.1 Junction definitions: (a) Location of the metallurgical junction, (b) doping profile—a plot of the net doping versus position.

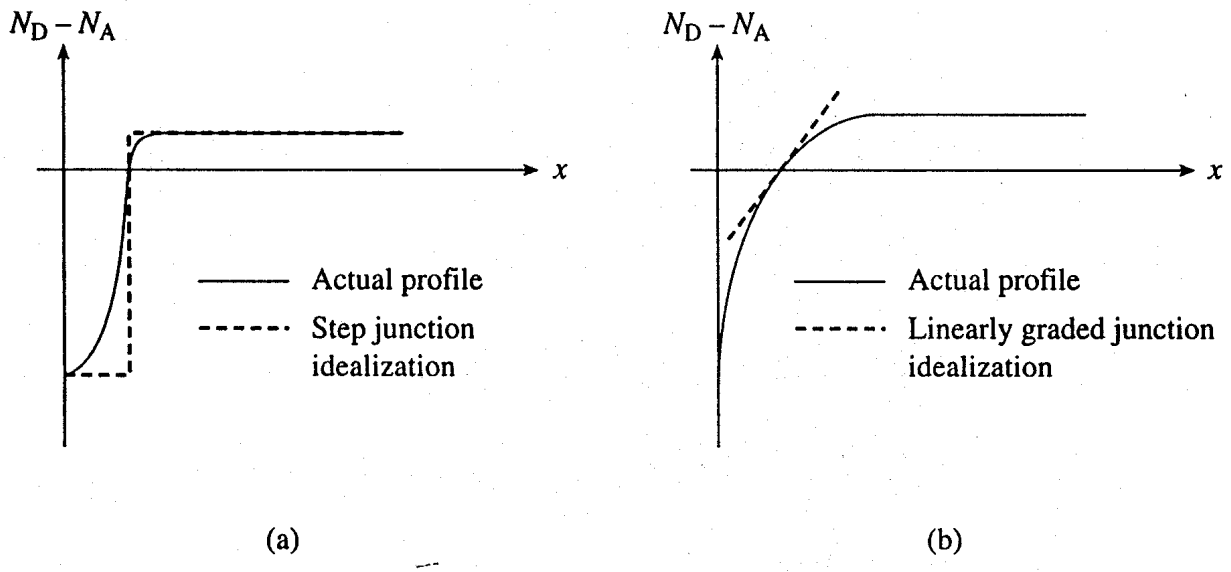

Figure 5.2 Idealized doping profiles: (a) Step junction, (b) linearly graded junction.

$N_D - N_A$ versus x plot as illustrated in Fig. 5.1(b). A plot of the net doping concentration as a function of position is referred to as the *doping profile.*

When incorporated into the analysis, the actual doping profiles created by the commonplace diffusion and ion implantation processes drastically complicate the mathematics. It becomes difficult to obtain and interpret results. Fortunately, only the doping variation in the immediate vicinity of the metallurgical junction is of prime importance. Surprisingly accurate results can be obtained using rather idealized doping profiles. The two most common idealizations are the *step junction* and the *linearly graded junction* profiles graphically defined in Fig. 5.2. The more appropriate of the two idealizations depends on the slope of the actual doping profile at the metallurgical junction and the background doping of the starting wafer. The step junction is an acceptable approximation to an ion-implantation or shallow diffusion into a lightly doped starting wafer, whereas the linearly graded profile would be more appropriate for deep diffusions into a moderate to heavily doped starting wafer. In most *pn* junction analyses presented herein, we arbitrarily invoke the step junction idealization to minimize the mathematical complexity of the analysis.

5.1.2 Poisson's Equation

Poisson's equation is a well-known relationship from Electricity and Magnetism. In semiconductor work it often constitutes the starting point in obtaining quantitative solutions for the electrostatic variables. The three-dimensional version appropriate for semiconductor analyses is

$$\nabla \cdot \mathscr{E} = \frac{\rho}{K_S \varepsilon_0} \tag{5.1}$$

In one-dimensional problems where $\mathscr{E} = \mathscr{E}_x$, Poisson's equation simplifies to

$$\boxed{\frac{d\mathscr{E}}{dx} = \frac{\rho}{K_S \varepsilon_0}} \tag{5.2}$$

K_S is the semiconductor dielectric constant and ε_0 is the permittivity of free space. ρ, previously associated with resistivity, is understood to be the charge density (charge/cm^3) in analyses involving the electrostatic variables. Assuming the dopants to be totally ionized, the charge density inside a semiconductor is given by

$$\boxed{\rho = q(p - n + N_D - N_A)} \tag{5.3}$$

Eq. (5.3) was originally presented as the first portion of Eq. (2.23) in deriving the charge neutrality relationship. The charge density is identically zero far from any surfaces inside a uniformly doped semiconductor in equilibrium. However, ρ is often nonzero and a function of position under less restrictive conditions.

Lastly note from Eq. (5.2) that ρ is proportional to $d\mathscr{E}/dx$ in one-dimensional problems. The general functional form of ρ versus x can therefore be deduced from an $\mathscr{E}-x$ plot by simply noting the slope of the plot as a function of position.

5.1.3 Qualitative Solution

Prior to performing a quantitative analysis, it is always useful to have a general idea as to the expected form of the solution. Based on the Subsection 3.2.4 discussion leading to the derivation of the Einstein relationship, we already know there should be band bending and an internal electric field associated with the inherently nonuniform doping of a *pn* junction diode. Let us assume a one-dimensional step junction and equilibrium conditions in seeking to determine the general functional form of the potential, electric field, and charge density inside the diode.

Our approach will be to first construct the energy band diagram for a *pn* junction diode under equilibrium conditions and then to utilize previously established procedures in deducing the electrostatic variables. For the assumed step junction it is reasonable to expect regions far removed from the metallurgical junction to be identical in character to an isolated, uniformly doped semiconductor. Thus, the energy band diagrams for the regions far removed from the junction are concluded to be of the simple form shown in Fig. 5.3(a). Under equilibrium conditions we know in addition that the Fermi level is a constant independent of position. This leads to Fig. 5.3(b), where the diagrams of Fig. 5.3(a) are properly aligned to the position-independent Fermi level. The missing near-junction portion of the Fig. 5.3(b) diagram is completed in Fig. 5.3(c) by connecting the E_c, E_i, and E_v endpoints on the two sides of the junction. Although the exact form of the band bending near the

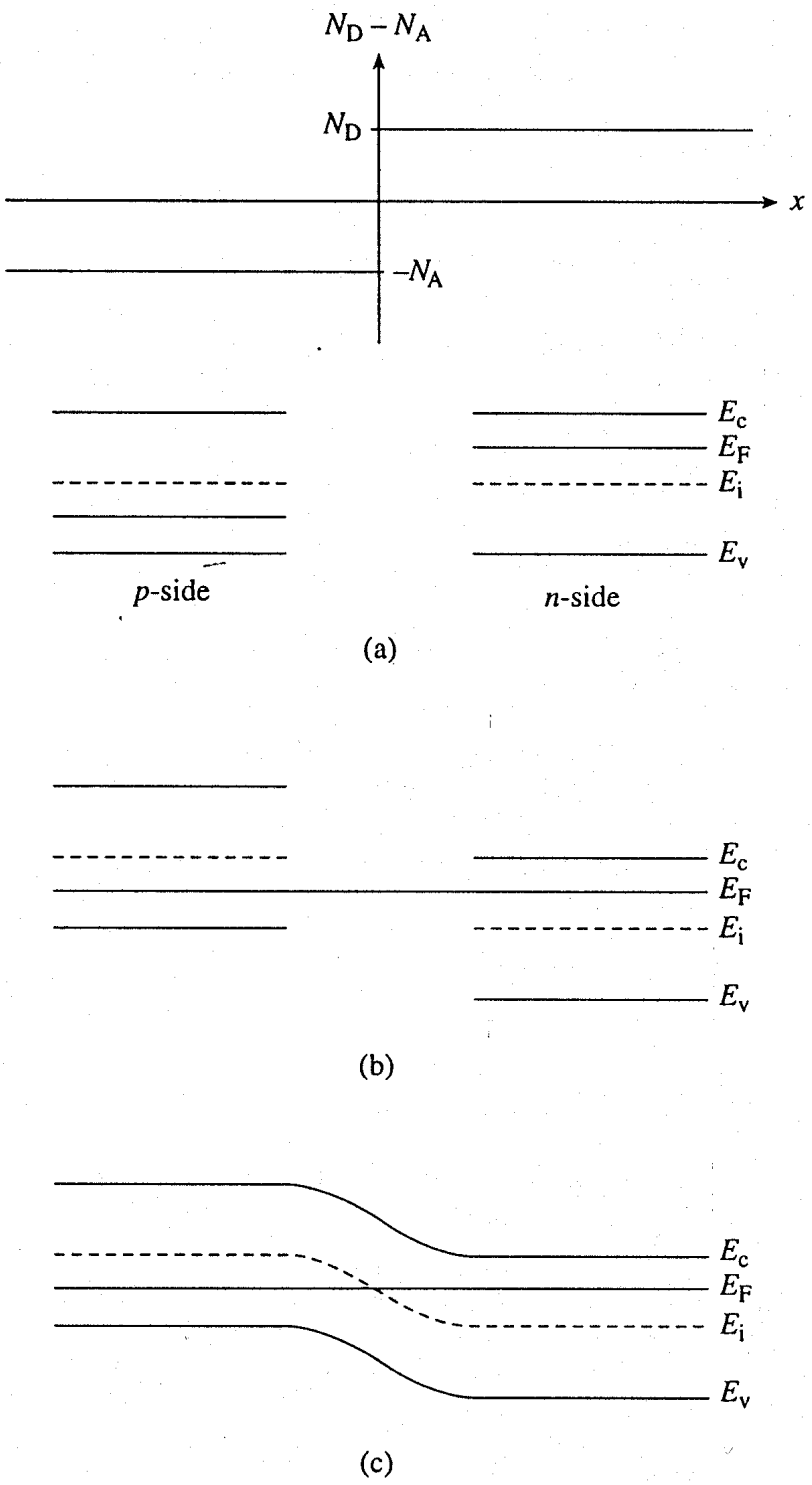

Figure 5.3 Step-by-step construction of the equilibrium energy band diagram for a *pn* junction diode. (a) Assumed step junction profile and energy band diagrams for the semiconductor regions far removed from the metallurgical junction. (b) Alignment of the part (a) diagrams to the position-independent Fermi level. (c) The completed energy band diagram.

metallurgical boundary is not known, it is reasonable to assume the variation is monotonic in nature, with a zero slope at the two ends of the central region. Figure 5.3(c) is of course the desired equilibrium energy band diagram for a *pn* junction diode.

It is now a relatively simple matter to deduce the functional form of the electrostatic variables. For one, referring to Subsection 3.1.5 on band bending, the V versus x relationship must have the same functional form as the "upside-down" of E_c (or E_i or E_v). This leads to the V versus x dependence sketched in Fig. 5.4(b) with V arbitrarily set equal to zero on the far p-side of the junction. Next, the $\mathscr{E}$ versus x dependence shown in Fig. 5.4(c) is obtained by recording the graphical derivative of E_c as a function of position.† Finally, the general functional form of ρ versus x sketched in Fig. 5.4(d) is deduced from the slope of the $\mathscr{E}-x$ plot.

Perhaps the most interesting features of the Fig. 5.4 solution are the voltage drop across the junction under equilibrium conditions and the appearance of charge near the metallurgical boundary. The "built-in" voltage (V_{bi}) will be given separate consideration in the next subsection. Of immediate interest is the region of charge near the junction pictured in Fig. 5.4(d). The question arises, Where does this charge come from? Answering this question provides considerable physical insight.

Suppose that the p- and n-regions were initially separated as pictured in Fig. 5.5(a). Charge neutrality is assumed to prevail in the isolated, uniformly doped semiconductors. In the p-material the positive hole charges, the $\oplus$'s in Fig. 5.5, balance the immobile acceptor-site charges shown as $\boxminus$'s in Fig. 5.5. Likewise, in the n-material the electronic charge ($\ominus$) everywhere balances the immobile charge associated with the ionized donors ($\boxplus$). Next suppose a structurally perfect connection is made between the p and n materials as envisioned in Fig. 5.5(b). Naturally, since there are many more holes on the p-side than on the n-side, holes begin to diffuse from the p-side to the n-side an instant after the connection is made. Similarly, electrons diffuse from the n-side to the p-side of the junction. Although the electrons and holes can move to the opposite side of the junction, the donors and acceptors are fixed in space. Consequently, the diffusing away of the carriers from the near-vicinity of the junction leaves behind an unbalanced dopant site charge as shown in Fig. 5.5(c). This is the source of the charge around the metallurgical junction, nicely correlating with the previously deduced ρ versus x dependence redrawn in Fig. 5.5(d). The near-vicinity of the metallurgical junction where there is a significant nonzero charge is called the *space charge region* or *depletion region.* The latter name follows from the fact that the carrier concentrations in the region are greatly reduced or depleted. We should also mention that the build-up of charge and the associated electric field continues until the diffusion of carriers across the junction is precisely balanced by the carrier drift. The individual carrier diffusion and drift components must of course cancel to make J_N and J_P separately zero under equilibrium conditions.

---

† Actually, from the Fig. 5.4(a) energy band diagram, one can conclude only that the magnitude of $\mathscr{E}$ first increases from zero on the p-side of the junction, reaches a maximum near the metallurgical boundary, and then decreases again to zero far on the n-side of the junction. The pseudo-linear dependence sketched in Fig. 5.4(c) reflects an advance knowledge of the quantitative solution.

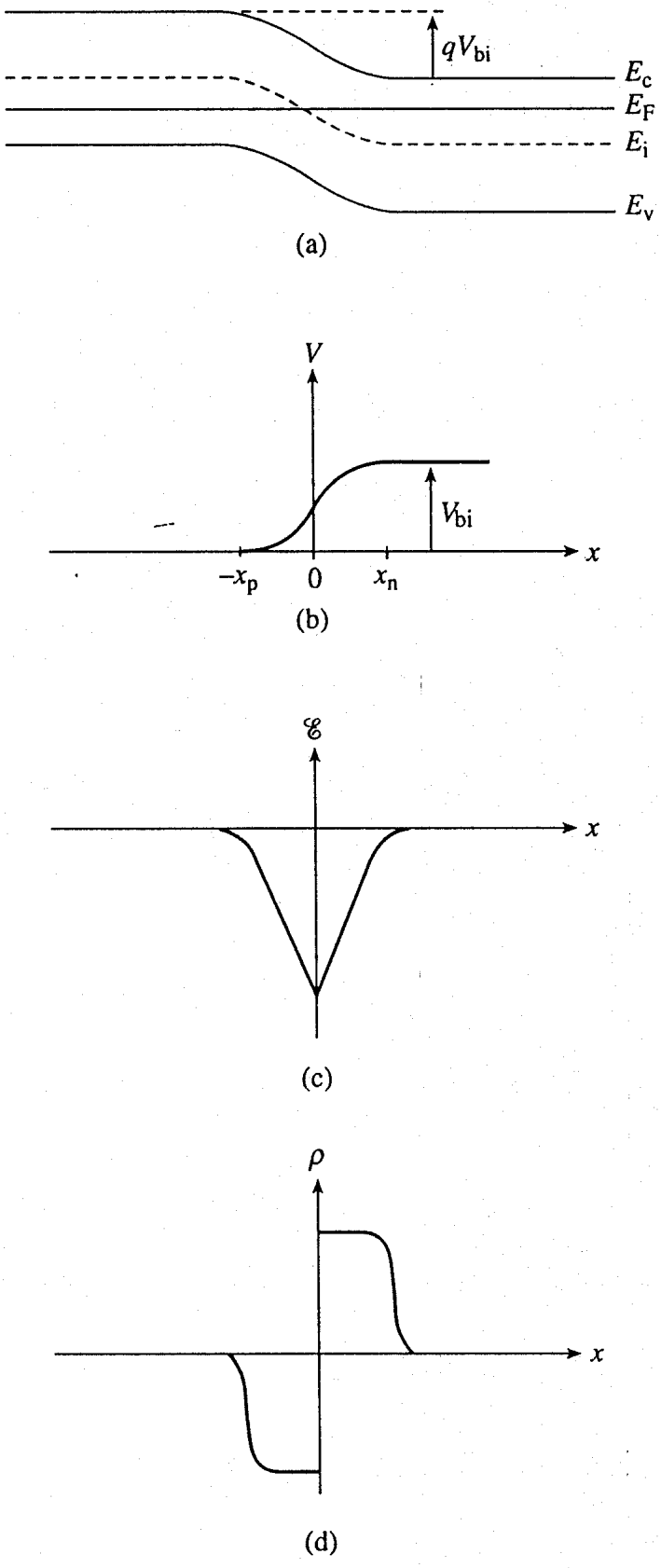

Figure 5.4 General functional form of the electrostatic variables in a *pn* junction under equilibrium conditions. (a) Equilibrium energy band diagram. (b) Electrostatic potential, (c) electric field, and (d) charge density as a function of position.

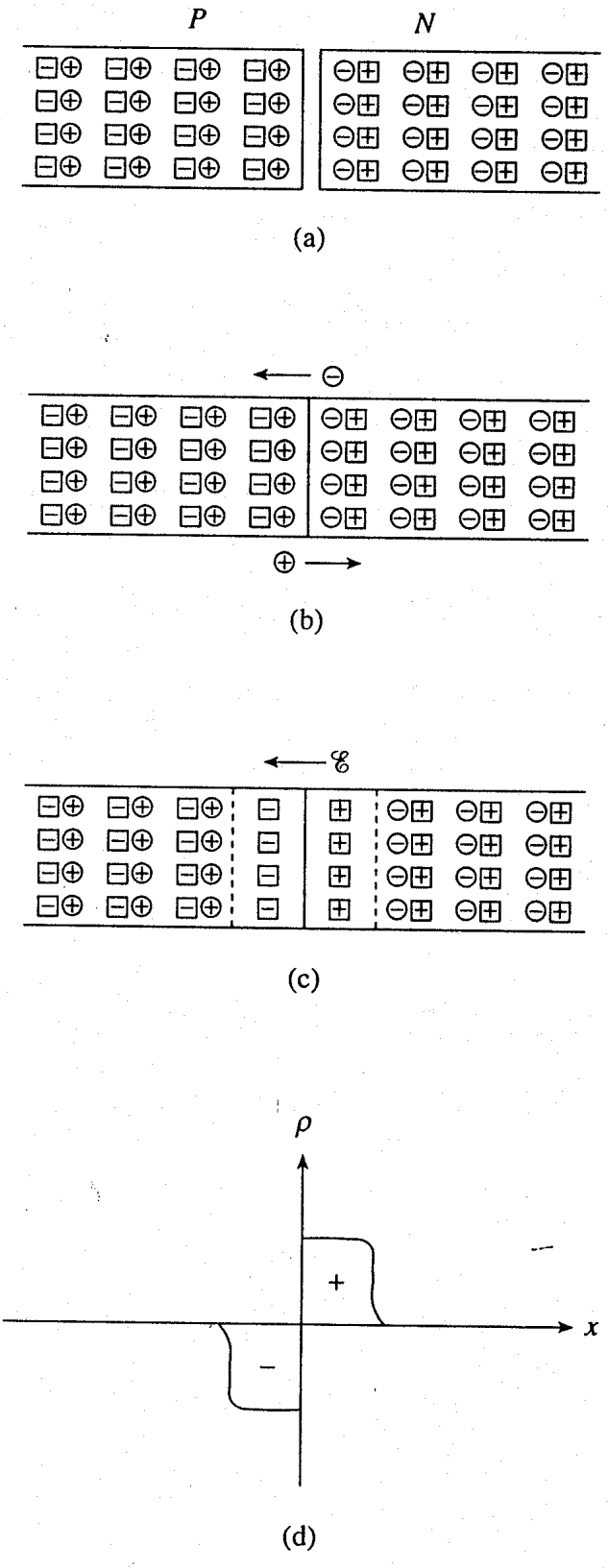

Figure 5.5 Conceptual *pn* junction formation and associated charge redistribution. (a) Isolated *p* and *n* regions. (b) Electrons and holes diffuse to the opposite side of the junction moments after joining the *p* and *n* regions. (c) Charge redistribution completed and equilibrium conditions re-established. (d) Previously deduced charge density versus position. (⊕–holes, ⊟–ionized acceptors, ⊖–electrons, and ⊞–ionized donors.)

5.1.4 The Built-in Potential (V_{bi})

The voltage drop across the depletion region under equilibrium conditions, known as the built-in potential (V_{bi}), is a junction parameter of sufficient importance to merit further consideration. We are particularly interested in establishing a computational relationship for V_{bi}. Working toward the stated goal, we consider a nondegenerately-doped *pn* junction maintained under equilibrium conditions with $x = 0$ positioned at the metallurgical boundary. The ends of the equilibrium depletion region are taken to occur at $-x_p$ and x_n on the *p*- and *n*-sides of the junction respectively (see Fig. 5.4b).

Proceeding with the derivation, we know

$$\mathscr{E} = -\frac{dV}{dx} \tag{5.4}$$

Integrating across the depletion region gives

$$-\int_{-x_p}^{x_n} \mathscr{E}\, dx = \int_{V(-x_p)}^{V(x_n)} dV = V(x_n) - V(-x_p) = V_{bi} \tag{5.5}$$

Furthermore, under equilibrium conditions,

$$J_N = q\mu_n n\mathscr{E} + qD_N \frac{dn}{dx} = 0 \tag{5.6}$$

Solving for $\mathscr{E}$ in Eq. (5.6) and making use of the Einstein relationship, we obtain

$$\mathscr{E} = -\frac{D_N}{\mu_n}\frac{dn/dx}{n} = -\frac{kT}{q}\frac{dn/dx}{n} \tag{5.7}$$

Substituting Eq. (5.7) into Eq. (5.5), and completing the integration then yields

$$V_{bi} = -\int_{-x_p}^{x_n} \mathscr{E}\, dx = \frac{kT}{q}\int_{n(-x_p)}^{n(x_n)} \frac{dn}{n} = \frac{kT}{q}\ln\left[\frac{n(x_n)}{n(-x_p)}\right] \tag{5.8}$$

For the specific case of a nondegenerately doped step junction where N_D and N_A are the *n*- and *p*-side doping concentrations, one identifies

$$n(x_n) = N_D \tag{5.9a}$$

$$n(-x_p) = \frac{n_i^2}{N_A} \tag{5.9b}$$

and therefore

$$\boxed{V_{bi} = \frac{kT}{q} \ln\left(\frac{N_A N_D}{n_i^2}\right)} \tag{5.10}$$

It is useful to perform a sample computation to gauge the relative magnitude of the built-in voltage. Choosing $N_A = N_D = 10^{15}/\text{cm}^3$ and a Si diode maintained at 300 K, one computes $V_{bi} = (0.0259)\ln(10^{30}/10^{20}) \cong 0.6$ V. This is a typical result. In nondegenerately doped diodes $V_{bi} < E_G/q$, or V_{bi} is less than the band gap energy converted to volts. Nondegenerately doped Ge, Si, and GaAs diodes maintained at room temperature exhibit a V_{bi} less than 0.66 V, 1.12 V, and 1.42 V, respectively.

The relationship between V_{bi} and E_G alluded to in the preceding paragraph is nicely explained by an alternative V_{bi} derivation based on the energy band diagram. Referring to Figs. 5.4(a) and (b), we note

$$V_{bi} = V(x_n) - V(-x_p) \tag{5.11a}$$

$$= \frac{1}{q}[E_c(-x_p) - E_c(x_n)] = \frac{1}{q}[E_i(-x_p) - E_i(x_n)] \tag{5.11b}$$

or

$$V_{bi} = \frac{1}{q}[(E_i - E_F)_{\text{p-side}} + (E_F - E_i)_{\text{n-side}}] \tag{5.12}$$

Clearly, for a nondegenerately doped diode both $(E_i - E_F)_{\text{p-side}}$ and $(E_F - E_i)_{\text{n-side}}$ are less than $E_G/2$, making $V_{bi} < E_G/q$. Moreover, in a nondegenerately doped step junction under equilibrium conditions,

$$(E_i - E_F)_{\text{p-side}} = kT \ln(N_A/n_i) \tag{5.13a}$$

$$(E_F - E_i)_{\text{n-side}} = kT \ln(N_D/n_i) \tag{5.13b}$$

Substituting Eqs. (5.13) into Eq. (5.12) and simplifying yields Eq. (5.10). Note that, while Eqs. (5.13) and hence Eq. (5.10) are valid only for nondegenerate dopings, there are no doping-related restrictions on the validity of Eq. (5.12).

(C) Exercise 5.1

P: Most real diodes are very heavily doped on one side of the junction. In computing the built-in voltage of p^+-n and n^+-p step junctions, it is common practice to assume that the Fermi level on the heavily doped side is positioned at the band edge; i.e., $E_F = E_v$ in a p^+ material and $E_F = E_c$ in an n^+ material. Making the cited assumption, compute and plot V_{bi} as a function of the doping (N_A or N_D) on the lightly doped side of Si p^+-n and n^+-p step junctions maintained at 300 K. The plot is to cover the range $10^{14}/cm^3 \leq N_A$ or $N_D \leq 10^{17}/cm^3$.

S: Specifically considering a p^+-n junction, we can write

$$(E_i - E_F)_{p\text{-side}} \text{ assumed} = E_i - E_v = E_G/2$$

$$(E_F - E_i)_{n\text{-side}} = kT \ln(N_D/n_i)$$

Substituting into Eq. (5.12), which is valid for arbitrary doping levels, we rapidly conclude

$$V_{bi} = \frac{E_G}{2q} + \frac{kT}{q} \ln\left(\frac{N_D}{n_i}\right)$$

For n^+-p junctions, N_A simply replaces N_D, yielding a computationally equivalent relationship. The V_{bi} computational program and resultant plot (Fig. E5.1) follow:

MATLAB program script...

```
%Vbi Computation (p+/n and n+/p junctions)

%Constants
EG=1.12;
kT=0.0259;
ni=1.0e10;

%Computation
ND=logspace(14,17);
Vbi=EG/2+kT.*log(ND./ni);

%Plotting
close
semilogx(ND,Vbi); grid
axis([1.0e14 1.0e17 0.75 1])
xlabel('NA or ND (cm-3)'); ylabel('Vbi (volts)')
text(1e16,0.8,'Si, 300K')
text(1e16,0.78,'p+/n and n+/p diodes')
```

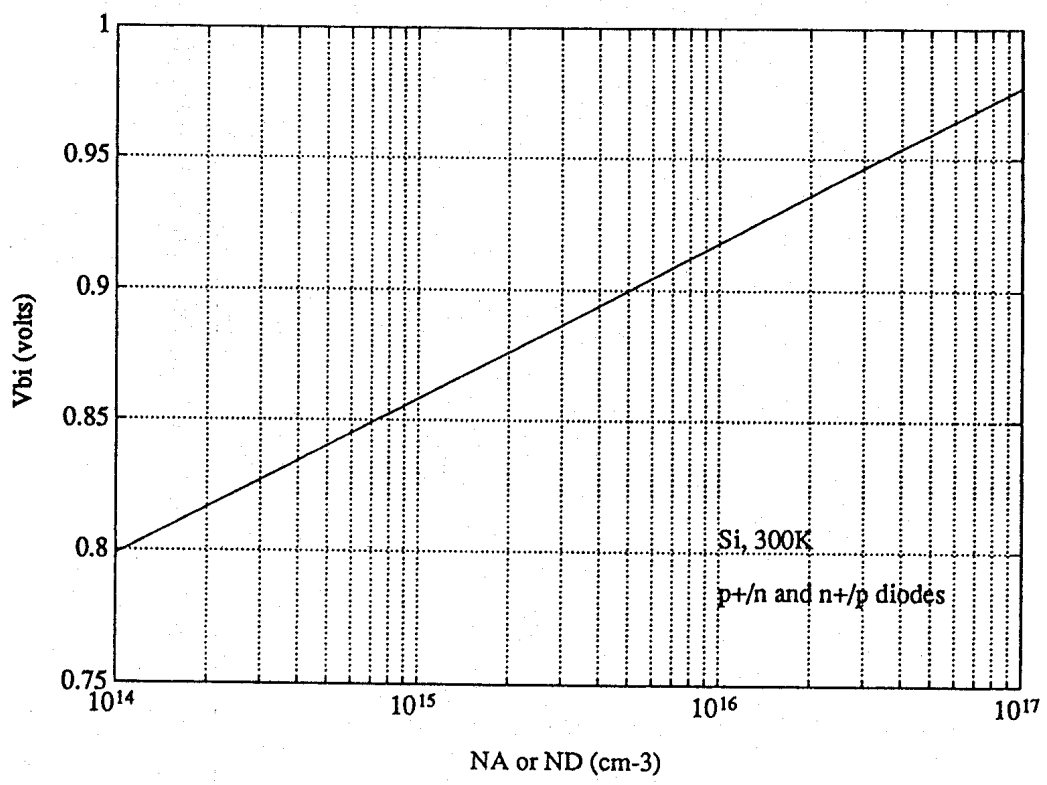

Figure E5.1 Built-in voltage in Si p^+-n and n^+-p step junction diodes at 300 K.

5.1.5 The Depletion Approximation

To obtain a quantitative solution for the electrostatic variables, it will be necessary to solve Poisson's equation. The depletion approximation facilitates obtaining closed-form solutions to the equation. Appearing in a myriad of device analyses, the depletion approximation is far and away the most important and most widely encountered of the simplifying approximations used in the modeling of devices.

To understand why the depletion approximation is introduced, consider the one-dimensional Poisson equation rewritten as Eq. (5.14). The doping profile, $N_D - N_A$, appearing in the equation

$$\frac{d\mathscr{E}}{dx} = \frac{\rho}{K_S \varepsilon_0} = \frac{q}{K_S \varepsilon_0}(p - n + N_D - N_A) \tag{5.14}$$

is assumed to be known. However, to write down ρ as a function of x, solve the differential equation for $\mathscr{E}$ versus x, and eventually obtain V versus x, one must also have explicit expressions for the carrier concentrations as a function of x. Unfortunately, the carrier concentrations in $\mathscr{E} \neq 0$ regions, like the *pn* junction depletion region, are not specified prior to solving Poisson's equation. Rather, p and n in the depletion region are functions of the potential as is obvious from an examination of the Fig. 5.4(a) energy band diagram. Although exact closed-form (usually complex) solutions do exist in certain instances, the

depletion approximation provides a simple, nearly universal way of obtaining approximate solutions without prior knowledge of the carrier concentrations.

We have already established the basis for the depletion approximation. A prominent feature of the qualitative solution was the appearance of a nonzero charge density straddling the metallurgical junction. This charge arises because the carrier numbers are reduced by diffusion across the junction. The carrier "depletion" tends to be greatest in the immediate vicinity of the metallurgical boundary and then tails off as one proceeds away from the junction. The depletion approximation introduces an idealization of the actual charge distribution. The approximation has two components that can be stated as follows: (1) The carrier concentrations are assumed to be negligible compared to the net doping concentration in a region $-x_p \leq x \leq x_n$ straddling the metallurgical junction. (2) The charge density outside the depletion region is taken to be identically zero. The depletion approximation is summarized pictorially in Fig. 5.6(a) and is illustrated assuming a step junction in

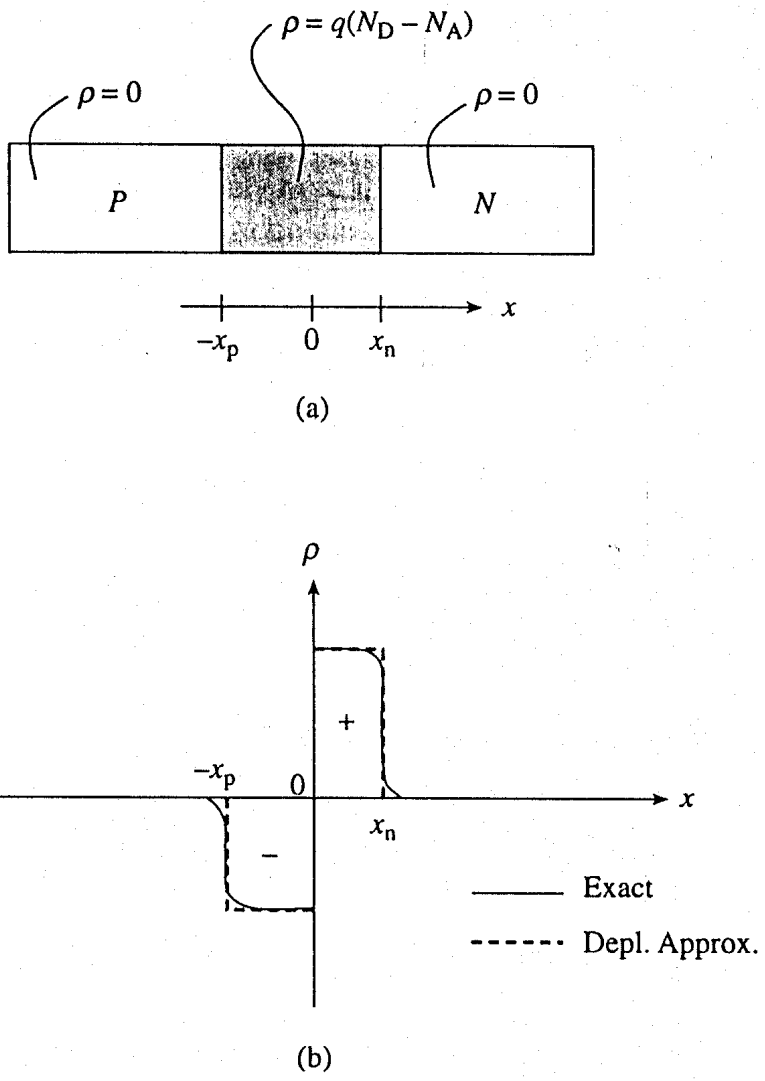

Figure 5.6 (a) Pictorial summary of the depletion approximation. (b) Illustration of the approximation as applied to a step junction.

Fig. 5.6(b). When the depletion approximation is invoked, the one-dimensional Poisson equation simplifies to

$$\frac{d\mathscr{E}}{dx} \cong \begin{cases} \dfrac{q}{K_S \varepsilon_0}(N_D - N_A) & \ldots -x_p \leq x \leq x_n \quad (5.15a) \\ 0 & \ldots x \leq -x_p \text{ and } x \geq x_n \quad (5.15b) \end{cases}$$

Note that, except for the values of $-x_p$ and x_n, the charge density is totally specified by invoking the depletion approximation. Moreover, the charge density will have precisely

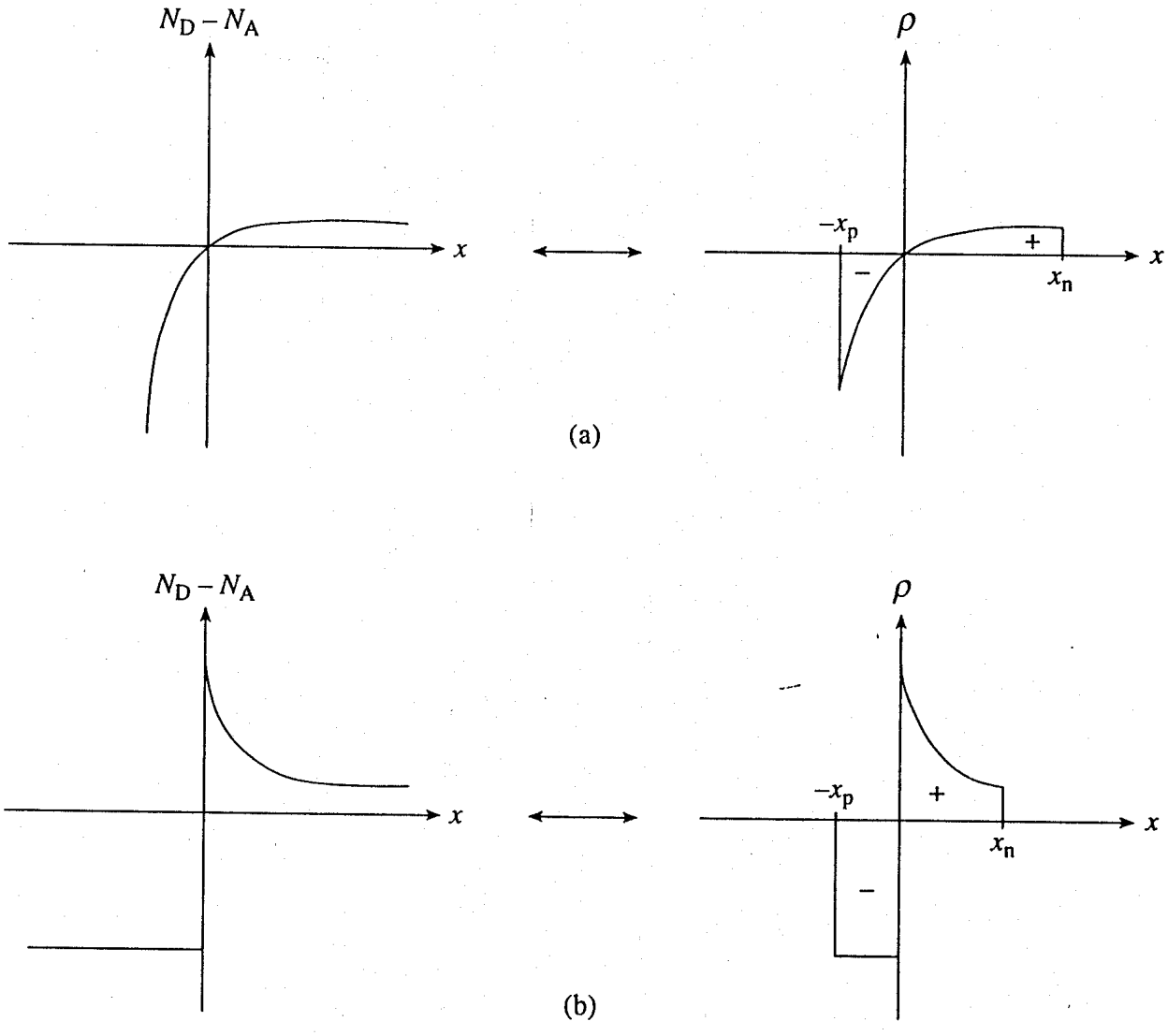

Figure 5.7 Relationship between the doping profile and the charge density based on the depletion approximation. (a) and (b) are two separate examples.

the same functional form as $N_D - N_A$ within the depletion region. Figure 5.7 is presented to emphasize this last point by showing the ρ versus x plots associated with sample doping profiles of a moderately complex nature.

5.2 QUANTITATIVE ELECTROSTATIC RELATIONSHIPS

With the preliminaries out of the way, we proceed to the main event: development of quantitative relationships for the electrostatic variables. The development primarily deals with the step junction and is presented in detail not only to obtain the desired relationships but also to establish the derivational procedures that can be applied to other doping profiles. We begin by carefully specifying the system under analysis, turn to the step junction under equilibrium conditions, and then consider the modifications required when there is an applied bias. The section concludes with a concise derivation and examination of the electrostatic relationships appropriate for a linearly graded junction.

5.2.1 Assumptions/Definitions

Major features of the *pn* junction diode subject to analysis are identified in Fig. 5.8. All variables are taken to be functions only of x, the coordinate normal to the semiconductor surface. The device is thus said to be "one-dimensional"; obvious two-dimensional effects associated with the lateral ends of a real device are assumed to be negligible. For the electrostatic analysis, $x = 0$ is positioned at the metallurgical boundary. External contacts to the ends of the diode are specified to be "ohmic" in nature. By definition, a negligible portion of an externally applied voltage appears across an ohmic contact. Note that the

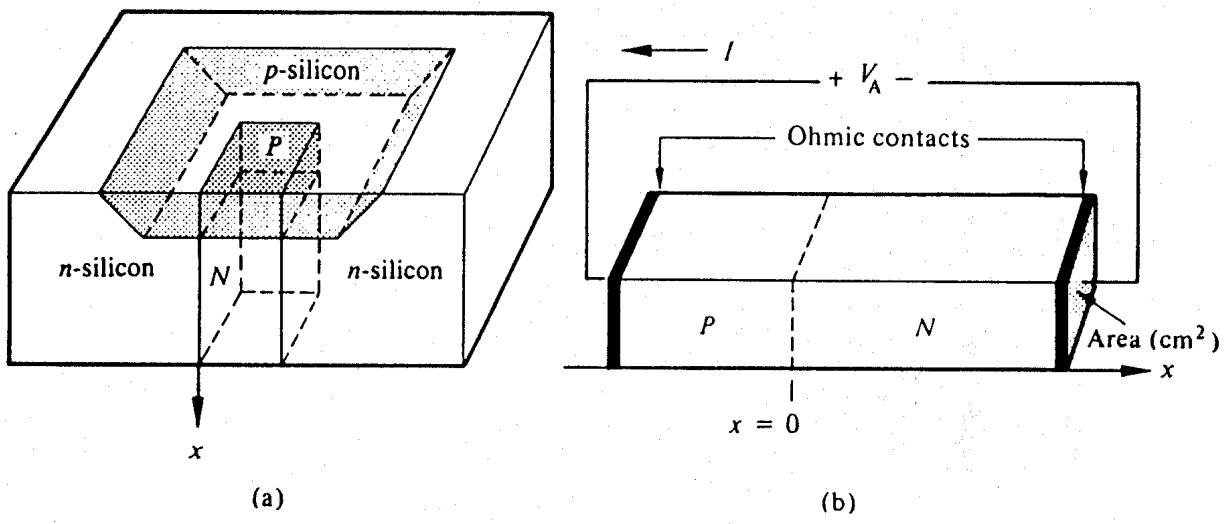

Figure 5.8 (a) Sketch of a physical diode. (b) One-dimensional diode subject to analysis including the applied voltage, coordinate, and contact specifications.

symbol V_A is used for the applied voltage. The subscript A distinguishes the applied voltage from the internal junction voltage. In the initial development V_A is set equal to zero, or equivalently, the device is assumed to be in equilibrium.

5.2.2 Step Junction with $V_A = 0$

Solution for ρ

We consider a step junction under equilibrium conditions. N_A is drawn greater than N_D in the Fig. 5.9(a) sketch of the doping profile for the sake of illustration. As summarized in Fig. 5.9(b), invoking the depletion approximation yields the charge density solution

$$\rho = \begin{cases} -qN_A & \ldots -x_p \le x \le 0 \quad (5.16a) \\ qN_D & \ldots 0 \le x \le x_n \quad (5.16b) \\ 0 & \ldots x \le -x_p \text{ and } x \ge x_n \quad (5.16c) \end{cases}$$

The values of x_n and x_p are not known at this point but will be determined later in the analysis.

Solution for $\mathscr{E}$

Substituting the charge density solution into Poisson's equation gives the equations to be solved for the electric field.

$$\frac{d\mathscr{E}}{dx} = \begin{cases} -qN_A/K_S\varepsilon_0 & \ldots -x_p \le x \le 0 \quad (5.17a) \\ qN_D/K_S\varepsilon_0 & \ldots 0 \le x \le x_n \quad (5.17b) \\ 0 & \ldots x \le -x_p \text{ and } x \ge x_n \quad (5.17c) \end{cases}$$

$\mathscr{E} = 0$ far from the metallurgical boundary and therefore $\mathscr{E} = 0$ everywhere outside of the depletion region. Since $\mathscr{E}$ must also vanish right at the edges of the depletion region, $\mathscr{E} = 0$ at $x = -x_p$ and $\mathscr{E} = 0$ at $x = x_n$ respectively become the boundary conditions for the (5.17a) and (5.17b) differential equations. Separating variables and integrating from the depletion region edge to an arbitrary point x, one obtains for the p-side of the depletion region

$$\int_0^{\mathscr{E}(x)} d\mathscr{E}' = -\int_{-x_p}^{x} \frac{qN_A}{K_S\varepsilon_0} dx' \quad (5.18)$$

or

$$\mathscr{E}(x) = -\frac{qN_A}{K_S\varepsilon_0}(x_p + x) \quad \ldots -x_p \le x \le 0 \quad (5.19)$$

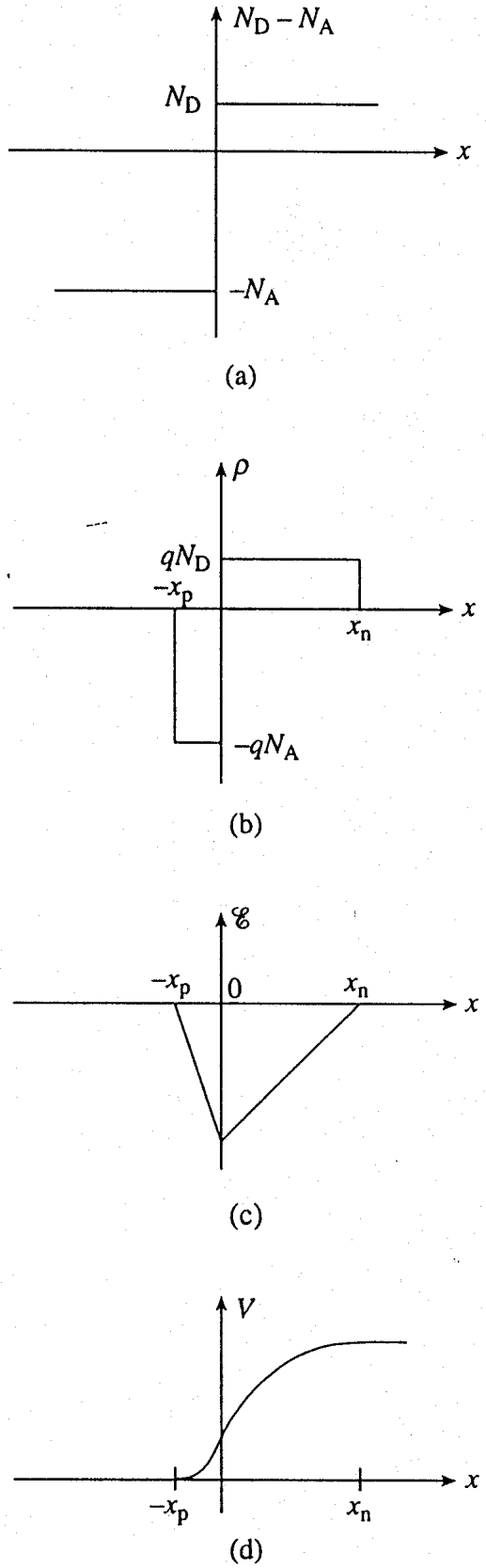

Figure 5.9 Step junction solution. Depletion approximation based quantitative solution for the electrostatic variables in a *pn* step junction under equilibrium conditions ($V_A = 0$). (a) Step junction profile. (b) Charge density, (c) electric field, and (d) electrostatic potential as a function of position.

Similarly on the n-side

$$\int_{\mathscr{E}(x)}^{0} d\mathscr{E}' = \int_{x}^{x_n} \frac{qN_D}{K_S \varepsilon_0} dx' \tag{5.20}$$

or

$$\mathscr{E}(x) = -\frac{qN_D}{K_S \varepsilon_0}(x_n - x) \qquad \ldots 0 \leq x \leq x_n \tag{5.21}$$

The electric field solution is plotted in Fig. 5.9(c). This result is of course consistent with the qualitative solution sketched in Fig. 5.4(c). Within the depletion region the field is always negative and exhibits a linear variation with position. It should be noted that in constructing Fig. 5.9(c) the electric field was taken to be continuous at $x = 0$; the p- and n-side solutions were simply matched at the metallurgical boundary. From Electricity and Magnetism, we know the electric field will be continuous across a boundary as long as a sheet of charge does not lie along the interface between the two regions. If the (5.19) and (5.21) expressions for the electric field are evaluated at $x = 0$ and equated, the continuity of the electric field is found to require

$$N_A x_p = N_D x_n \tag{5.22}$$

For those familiar with Gauss' law, the fact that $\mathscr{E} = 0$ outside the depletion region means the total charge within the depletion region must sum to zero, or the minus charge on the p-side of the junction must balance the plus charge on the n-side of the junction. Previous charge density plots (Figs. 5.4–5.7) have all been drawn with this fact in mind. Applied to the step junction ρ versus x plot in Fig. 5.9(b), the balance of charge requires the rectangular areas on the p- and n-sides of the junction to be equal, or $qN_A x_p = qN_D x_n$. Thus Eq. (5.22) may be viewed alternatively as a reflection of the fact that the total charge within the depletion region must sum to zero.

Solution for V

Since $\mathscr{E} = -dV/dx$, the electrostatic potential is obtained by solving

$$\frac{dV}{dx} = \begin{cases} \dfrac{qN_A}{K_S \varepsilon_0}(x_p + x) & \ldots -x_p \leq x \leq 0 \qquad (5.23a) \\ \dfrac{qN_D}{K_S \varepsilon_0}(x_n - x) & \ldots 0 \leq x \leq x_n \qquad (5.23b) \end{cases}$$

With the arbitrary reference potential set equal to zero at $x = -x_p$, and remembering the voltage drop is V_{bi} across the depletion region under equilibrium conditions, Eqs. (5.23a) and (5.23b) are respectively subject to the boundary conditions

$$V = 0 \quad \text{at} \quad x = -x_p \tag{5.24a}$$

$$V = V_{bi} \quad \text{at} \quad x = x_n \tag{5.24b}$$

Separating variables and integrating from the depletion region edge to an arbitrary point x, one obtains for the p-side of the depletion region

$$\int_0^{V(x)} dV' = \int_{-x_p}^{x} \frac{qN_A}{K_S \varepsilon_0}(x_p + x')\,dx' \tag{5.25}$$

or

$$V(x) = \frac{qN_A}{2K_S \varepsilon_0}(x_p + x)^2 \qquad \ldots -x_p \leq x \leq 0 \tag{5.26}$$

Similarly on the n-side of the junction

$$\int_{V(x)}^{V_{bi}} dV' = \int_{x}^{x_n} \frac{qN_D}{K_S \varepsilon_0}(x_n - x')\,dx' \tag{5.27}$$

or

$$V(x) = V_{bi} - \frac{qN_D}{2K_S \varepsilon_0}(x_n - x)^2 \qquad \ldots 0 \leq x \leq x_n \tag{5.28}$$

The electrostatic potential solution given by Eqs. (5.26) and (5.28) is plotted in Fig. 5.9(d). The V versus x dependence is quadratic in nature, with a concave curvature on the p-side of the junction and a convex curvature on the n-side of the junction. Paralleling the $\mathscr{E}$-field procedure, Fig. 5.9(d) was constructed simply by matching the p- and n-side solutions at $x = 0$. The assumed continuity of the electrostatic potential at $x = 0$ is justified because there is no dipole layer (closely spaced sheets of plus and minus charge) along the metallurgical boundary. Note that if the (5.26) and (5.28) expressions for the potential are evaluated at $x = 0$ and equated, one obtains

$$\frac{qN_A}{2K_S \varepsilon_0}x_p^2 = V_{bi} - \frac{qN_D}{2K_S \varepsilon_0}x_n^2 \tag{5.29}$$

Solution for x_n and x_p

The electrostatic solution is not complete until the values of x_n and x_p are determined. In the course of the development, we have already laid the groundwork for obtaining the n- and p-side depletion widths. Specifically, x_n and x_p are the only unknowns in Eqs. (5.22)

and (5.29). Eliminating x_p in Eq. (5.29) using Eq. (5.22) and solving the resulting equation for x_n rapidly yields

$$x_n = \left[\frac{2K_S\varepsilon_0}{q}\frac{N_A}{N_D(N_A + N_D)}V_{bi}\right]^{1/2} \tag{5.30a}$$

and

$$x_p = \frac{N_D x_n}{N_A} = \left[\frac{2K_S\varepsilon_0}{q}\frac{N_D}{N_A(N_A + N_D)}V_{bi}\right]^{1/2} \tag{5.30b}$$

It also follows that

$$W \equiv x_n + x_p = \left[\frac{2K_S\varepsilon_0}{q}\left(\frac{N_A + N_D}{N_A N_D}\right)V_{bi}\right]^{1/2} \tag{5.31}$$

W, the total width of the depletion region, better known simply as the *depletion width*, is often encountered in practical device computations.

Exercise 5.2

P: Perform a sample computation to gauge the size of W and $|\mathscr{E}|_{max}$ under equilibrium conditions. Specifically assume a Si step junction operated at 300 K with $N_A = 10^{17}/\text{cm}^3$ and $N_D = 10^{14}/\text{cm}^3$.

S: For the given junction,

$$V_{bi} = \frac{kT}{q}\ln\left(\frac{N_A N_D}{n_i^2}\right) = (0.0259)\ln\left[\frac{(10^{17})(10^{14})}{(10^{20})}\right] = 0.656\ \text{V}$$

Making use of Eqs. (5.30), one computes

$$x_n \cong \left[\frac{2K_S\varepsilon_0}{qN_D}V_{bi}\right]^{1/2} = \left[\frac{(2)(11.8)(8.85 \times 10^{-14})(0.656)}{(1.6 \times 10^{-19})(10^{14})}\right]^{1/2}$$

$$= 2.93 \times 10^{-4}\ \text{cm} = 2.93\ \mu\text{m}$$

$$x_p = \left(\frac{N_D}{N_A}\right)x_n = (10^{-3})x_n = 2.93 \times 10^{-7}\ \text{cm}$$

and

$$W = x_n + x_p \cong x_n = \boxed{2.93\ \mu\text{m}}$$

Also

$$|\mathscr{E}|_{max} = |\mathscr{E}(0)| = \frac{qN_D}{K_S\varepsilon_0}x_n = \frac{(1.6 \times 10^{-19})(10^{14})(2.93 \times 10^{-4})}{(11.8)(8.85 \times 10^{-14})}$$

$$= \boxed{4.49 \times 10^3 \text{ V/cm}}$$

W could have been computed directly using Eq. (5.31). However, we wished to make the additional point that in an asymmetrically doped junction ($N_A \gg N_D$ or $N_D \gg N_A$) the depletion region lies almost exclusively on the lightly doped side of the metallurgical boundary.

5.2.3 Step Junction with $V_A \neq 0$

The solution for the electrostatic variables must be extended to $V_A \neq 0$ operating conditions if it is to be of practical utility. One solution approach would be to pedantically repeat the derivations from the previous subsection with $V_A \neq 0$. Fortunately, there is an easier approach.

Consider the diode in Fig. 5.10 with a voltage $V_A \neq 0$ applied to the diode terminals. This voltage must be dropped somewhere inside the diode. However, in a well-made device a negligible portion of the applied voltage appears across the contacts to the device. Moreover, under low-level injection conditions (reasonable current levels) the resistive voltage drop across the quasineutral p- and n-regions extending from the contacts to the edges of the depletion region will also be negligible. The applied voltage must therefore be dropped across the depletion region. When $V_A > 0$, this externally imposed voltage drop *lowers* the potential on the n-side of the junction relative to the p-side of the junction. Conversely, when $V_A < 0$, the potential on the n-side increases relative to the p-side. In other words,

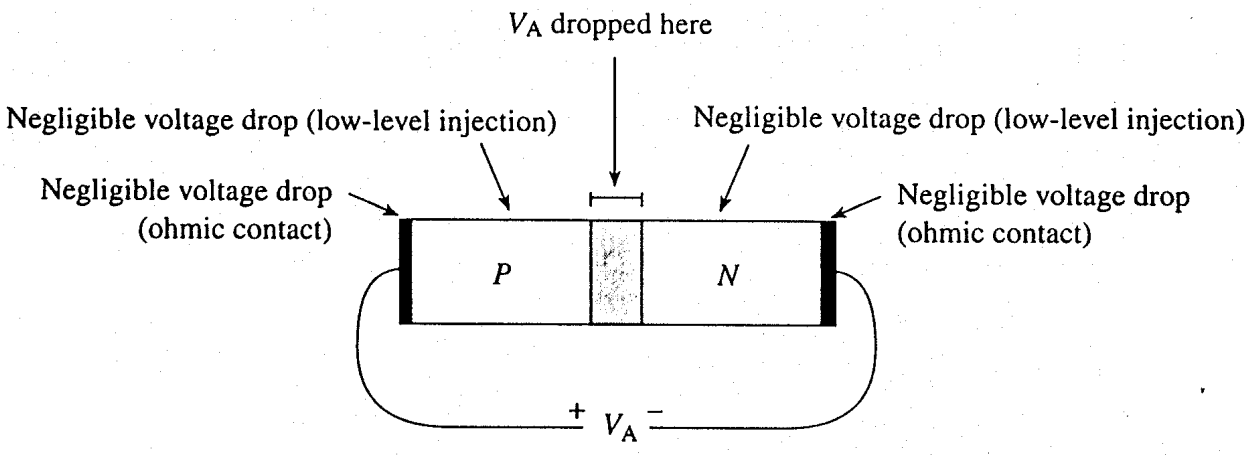

Figure 5.10 Voltage drops internal to a diode resulting from an externally applied voltage.

the voltage drop across the depletion region, and hence the boundary condition at $x = x_n$, becomes $V_{bi} - V_A$.

Since the only modification to the formation of the problem is a change in one boundary condition, the $V_A \neq 0$ electrostatic relationships can be extrapolated from the $V_A = 0$ relationships by simply replacing all explicit appearances of V_{bi} by $V_{bi} - V_A$. Making the indicated substitution yields the $V_A \neq 0$ solution for the electrostatic variables given in Eqs. (5.32)–(5.38).

For $-x_p \leq x \leq 0 \ldots$

$$\mathscr{E}(x) = -\frac{qN_A}{K_S\varepsilon_0}(x_p + x) \tag{5.32}$$

$$V(x) = \frac{qN_A}{2K_S\varepsilon_0}(x_p + x)^2 \tag{5.33}$$

$$x_p = \left[\frac{2K_S\varepsilon_0}{q}\frac{N_D}{N_A(N_A + N_D)}(V_{bi} - V_A)\right]^{1/2} \tag{5.34}$$

For $0 \leq x \leq x_n \ldots$

$$\mathscr{E}(x) = -\frac{qN_D}{K_S\varepsilon_0}(x_n - x) \tag{5.35}$$

$$V(x) = V_{bi} - V_A - \frac{qN_D}{2K_S\varepsilon_0}(x_n - x)^2 \tag{5.36}$$

$$x_n = \left[\frac{2K_S\varepsilon_0}{q}\frac{N_A}{N_D(N_A + N_D)}(V_{bi} - V_A)\right]^{1/2} \tag{5.37}$$

and

$$\boxed{W = \left[\frac{2K_S\varepsilon_0}{q}\left(\frac{N_A + N_D}{N_AN_D}\right)(V_{bi} - V_A)\right]^{1/2}} \tag{5.38}$$

To prevent an imaginary result, V_A is obviously restricted to $V_A \leq V_{bi}$ in Eqs. (5.34), (5.37), and (5.38). The formulation fails because a large current begins to flow, and the quasineutral region voltage drops cannot be neglected, when V_A approaches V_{bi}.

(C) Exercise 5.3

P: Construct a log-log plot of the depletion width (W) versus the impurity concentration (N_A or N_D) on the lightly doped side of Si p^+-n and n^+-p step junctions maintained at 300 K. Include curves for $V_A = 0.5$ V, 0 V, and -10 V covering the range $10^{14}/\text{cm}^3 \leq N_A$ or $N_D \leq 10^{17}/\text{cm}^3$.

S: The V_{bi} associated with the p^+-n and n^+-p step junctions is computed using the relationship established in Exercise 5.1. Also, with the junction asymmetrically doped, the doping factor in the Eq. (5.38) expression for W simplifies to

$$\frac{N_A + N_D}{N_A N_D} \cong \frac{1}{N_B}$$

where N_B is the doping (N_A or N_D) on the lightly doped side of the junction. The MATLAB program for the W versus doping computation and the program results (Fig. E5.3) follow:

MATLAB program script...

```
% This program calculates and plots the depletion width vs impurity
% concentration in Silicon p+/n and n+/p step junctions at 300K.
%
% Three plots are generated corresponding to VA = 0.5V, 0.0V, and -10V
%
%   The Vbi relationship employed is Vbi=(EG/2q)+(kT/q)ln(NB/ni)
%   where NB is the impurity concentration on the lightly doped side.

%Constants and Parameters
T=300;          % Temperature in Kelvin
k=8.617e-5;     % Boltzmann constant (eV/K)
e0=8.85e-14;    % permittivity of free space (F/cm)
q=1.602e-19;    % charge on an electron (coul)
KS=11.8;        % dielectric constant of Si at 300K
ni=1e10;        % intrinsic carrier conc. in Silicon at 300K (cm^-3)
EG=1.12;        % band gap of Silicon (eV)

%Choose variable values
NB=logspace(14,17);     % doping ranges from 1e14 to 1e17
VA=[0.5 0 -10];         % VA values set
```

```
%Depletion width calculation
Vbi=EG/2+k*T.*log(NB./ni);
W(1,:)=1.0e4*sqrt(2*KS*e0/q.*(Vbi-VA(1))./NB);
W(2,:)=1.0e4*sqrt(2*KS*e0/q.*(Vbi-VA(2))./NB);
W(3,:)=1.0e4*sqrt(2*KS*e0/q.*(Vbi-VA(3))./NB);

%Plot
close
loglog(NB, W,'-'); grid
axis([1.0e14 1.0e17 1.0e-1 1.0e1])
xlabel('NA or ND (cm^-3)')
ylabel('W (micrometers)')
set(gca,'DefaultTextUnits','normalized')
text(.38,.26,'VA=0.5V')
text(.38,.50,'VA=0')
text(.38,.76,'VA=-10V')
text(.77,.82,'Si,300K')
text(.77,.79,'p+/n and n+/p')
set(gca,'DefaultTextUnits','data')
```

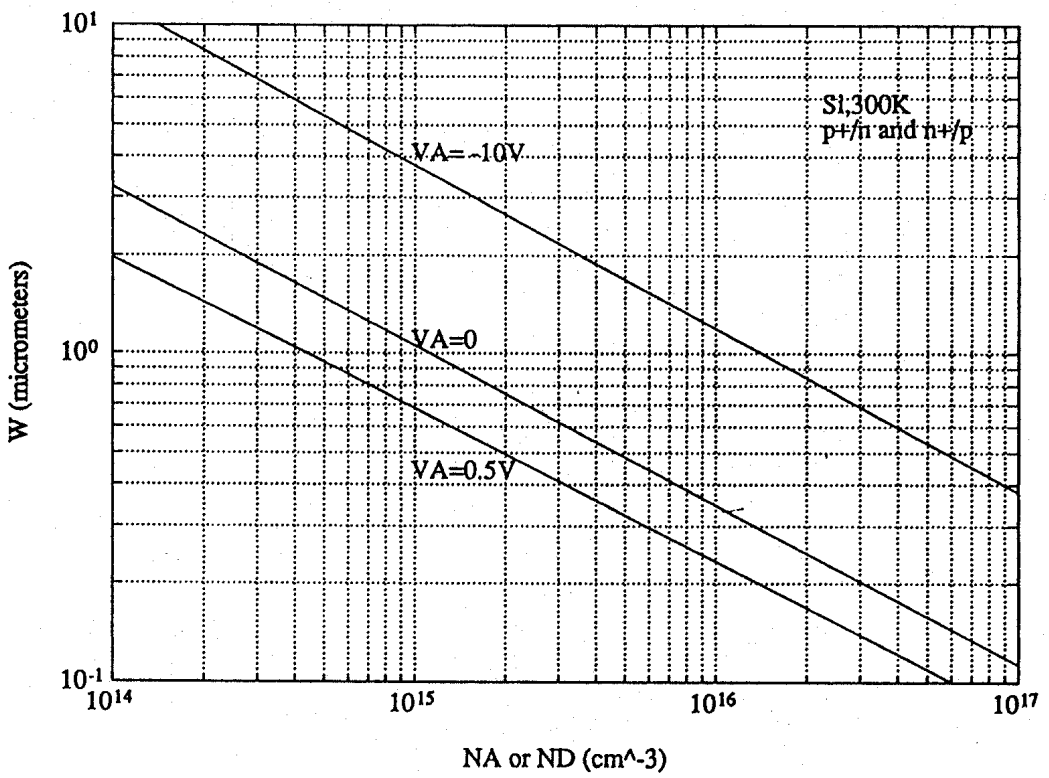

Figure E5.3 Depletion width at select applied biases as a function of doping (Si, p^+-n and n^+-p step junctions, 300 K).

5.2.4 Examination/Extrapolation of Results

Having expended considerable effort in establishing the results, it is reasonable to spend a few moments examining the results. We are particularly interested in how the electrostatic variables change as a function of the applied bias. Examining the (5.34) and (5.37) relationships for x_p and x_n, we conclude these widths decrease under forward biasing ($V_A > 0$) and increase under reverse biasing ($V_A < 0$). This conclusion is of course consistent with the Exercise 5.3 computation showing a smaller depletion width for $V_A > 0$ and a larger depletion width for $V_A < 0$. The changes in x_p and x_n likewise translate into changes in the electric field. As deduced from Eqs. (5.32) and (5.35), a smaller x_p and x_n under forward biases cause the $\mathscr{E}$-field to decrease everywhere inside the depletion region, while the larger x_p and x_n associated with reverse biases give rise to a larger $\mathscr{E}$-field. This conclusion is also reasonable from a physical standpoint. A decreased depletion width when $V_A > 0$ means less charge around the junction and a correspondingly smaller $\mathscr{E}$-field. $V_A < 0$, on the other hand, creates a larger space charge region and a bigger electric field. Similarly, the potential given by Eqs. (5.33) and (5.36) decreases at all points when $V_A > 0$ and increases at all points when $V_A < 0$. The potential hill shrinks in both size and x-extent under forward biasing, whereas reverse biasing gives rise to a wider and higher potential hill. The foregoing discussion is graphically summarized in Fig. 5.11.

In Subsection 3.1.5 we established a procedure for deducing the form of the electrostatic potential from a given energy band diagram. The procedure was applied in Subsection 5.1.3 to obtain the qualitative solution for the electrostatic potential inside a *pn* junction under equilibrium conditions. Having just described and envisioned (Fig. 5.11d) how the potential changes as a function of bias, we should be able to reverse the cited procedure to construct the energy band diagrams appropriate for a *pn* junction under forward and reverse bias. Specifically, we know what the energy band diagram looks like under equilibrium conditions (redrawn in Fig. 5.12a). Conceptually taking the upside-down of the potential plots and appropriately modifying the equilibrium energy band diagram—smaller depletion width and smaller hill for forward bias, larger depletion width and larger hill for reverse bias—yields the diagrams for forward and reverse bias respectively pictured in Figs. 5.12(b) and (c).

Several comments are in order concerning the $V_A \neq 0$ diagrams. For one, the Fermi level is omitted from the depletion region because the device is no longer in equilibrium and a single level cannot be used to describe the carrier concentrations in this region. In fact, the levels labeled E_{Fn} and E_{Fp}, occupying the former position of the Fermi level in the quasineutral regions, are actually majority-carrier quasi-Fermi levels. However, the deviation from equilibrium in the nondepleted portions of the diode is normally small, especially far from the junction, and it is therefore acceptable to continue using the E_F designation. Finally, by carefully inspecting the diagrams, it is readily established that

$$E_{Fp} - E_{Fn} = -qV_A \tag{5.39}$$

Equation (5.39) suggests one may conceive of the diode terminals as providing direct access to the p- and n-ends of the equilibrium Fermi level. Conceptually grabbing onto the

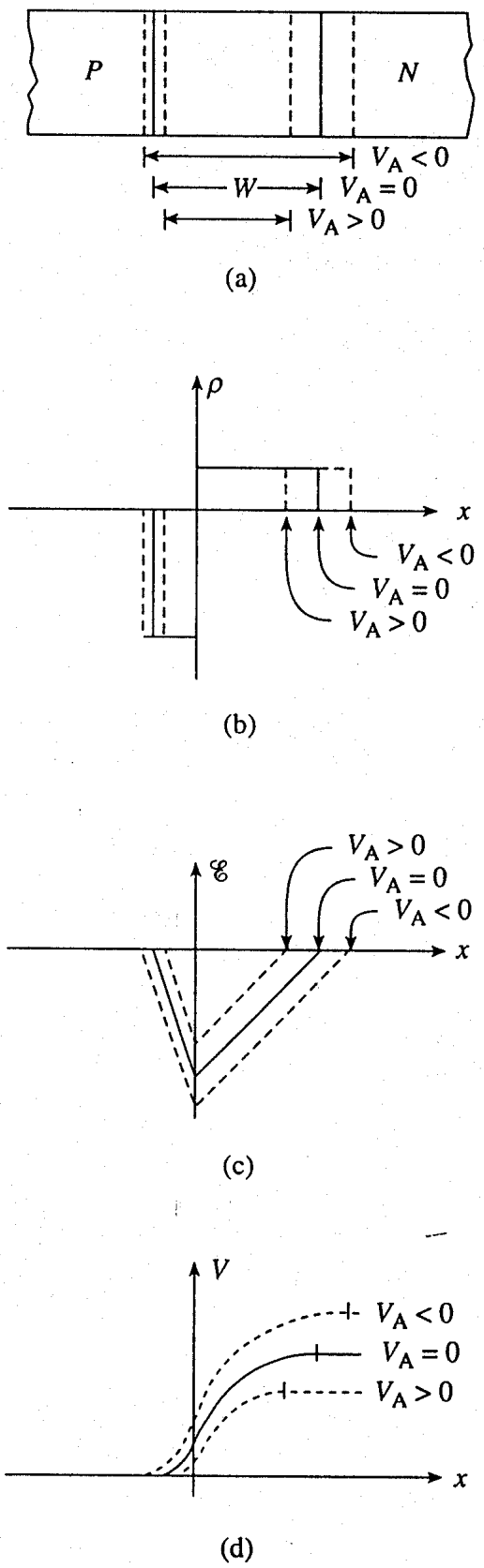

Figure 5.11 Effect of forward and reverse biasing on the (a) depletion width, (b) charge density, (c) electric field, and (d) electrostatic potential inside a *pn* junction diode.

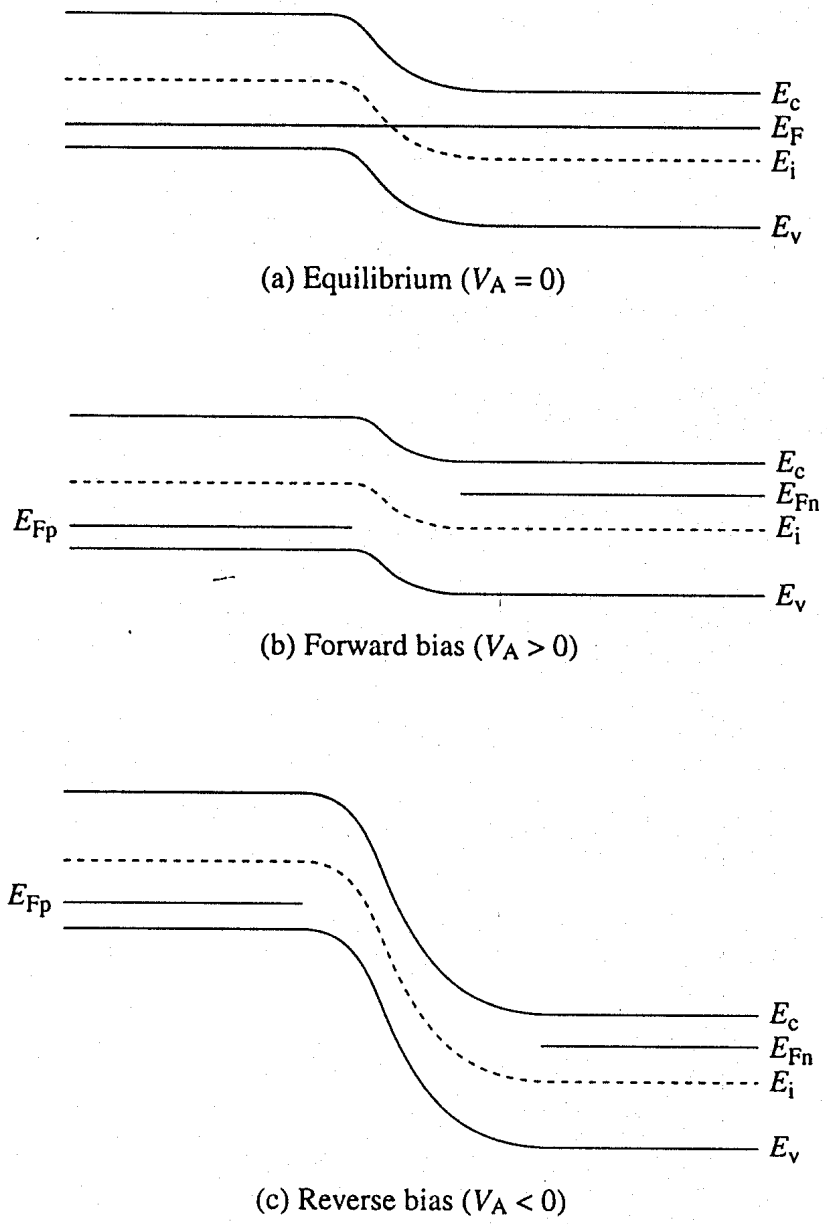

Figure 5.12 *pn* junction energy band diagrams. (a) Equilibrium ($V_A = 0$), (b) forward bias ($V_A > 0$), and (c) reverse bias ($V_A < 0$).

ends of the equilibrium Fermi level, one progresses from the equilibrium diagram to the forward bias diagram by moving the n-side upward by qV_A while holding the p-side fixed. Similarly, the reverse bias diagram is obtained from the equilibrium diagram by pulling the n-side Fermi level downward.

(C) Exercise 5.4

Once a quantitative relationship has been established for the electrostatic potential, it becomes possible to construct a fully dimensioned energy band diagram. The "Diagram Generator" program that follows draws the equilibrium energy band diagram

for a nondegenerately doped Si step junction maintained at room temperature. The user is prompted to input the p- and n-side doping concentrations. Run the program trying different N_A and N_D combinations. It is informative to include at least one combination each where $N_A \gg N_D$, $N_A \cong N_D$, and $N_A \ll N_D$. The asymmetrical junctions are of particular interest because the resultant "one-sided" diagrams differ from those normally included in textbooks. The user might also consider modifying the program so that it draws the energy band diagram for an arbitrary applied bias.

MATLAB program script...

```
% Equilibrium Energy Band Diagram Generator
%(Si, 300K, nondegenerately doped step junction)

%Constants
T=300;          % Temperature in Kelvin
k=8.617e-5;     % Boltzmann constant (eV/K)
e0=8.85e-14;    % permittivity of free space (F/cm)
q=1.602e-19;    % charge on an electron (coul)
KS=11.8;        % Dielectric constant of Si
ni=1.0e10;      % intrinsic carrier conc. in Silicon at 300K (cm^-3)
EG=1.12;        % Silicon band gap (eV)

%Control constants
xleft = -3.5e-4;     % Leftmost x position
xright = -xleft;     % Rightmost x position
NA=input ('Please enter p-side doping (cm^-3), NA = ');
ND=input ('Please enter n-side doping (cm^-3), ND = ');

%Computations
Vbi=k*T*log((NA*ND)/ni^2);
xN=sqrt(2*KS*e0/q*NA*Vbi/(ND*(NA+ND)));      % Depletion width n-side
xP=sqrt(2*KS*e0/q*ND*Vbi/(NA*(NA+ND)));      % Depletion width p-side
x = linspace(xleft, xright, 200);
Vx1=(Vbi-q*ND.*(xN-x).^2/(2*KS*e0).*(x<=xN)).*(x>=0);
Vx2=0.5*q*NA.*(xP+x).^2/(KS*e0).*(x>=-xP & x<0);
Vx=Vx1+Vx2;                                  % V as a function of x
VMAX = 3;                                    % Maximum Plot Voltage
EF=Vx(1)+VMAX/2-k*T*log(NA/ni);              % Fermi level

%Plot Diagram
close
plot (x, -Vx+EG/2+VMAX/2);
axis ([xleft xright 0 VMAX]);
axis ('off'); hold on
plot (x, -Vx-EG/2+VMAX/2);
```

```
plot (x, -Vx+VMAX/2,'w:');
plot ([xleft xright], [EF EF], 'w');
plot ([0 0], [0.15 VMAX-0.5], 'w--');
text(xleft*1.08,(-Vx(1)+EG/2+VMAX/2-.05),'Ec');
text(xright*1.02,(-Vx(200)+EG/2+VMAX/2-.05),'Ec');
text(xleft*1.08,(-Vx(1)-EG/2+VMAX/2-.05),'Ev');
text(xright*1.02,(-Vx(200)-EG/2+VMAX/2-.05),'Ev');
text(xleft*1.08,(-Vx(1)+VMAX/2-.05),'Ei');
text(xright*1.02, EF-.05,'EF');
set(gca,'DefaultTextUnits','normalized')
text(.18, 0,'p-side');
text(.47, 0, 'x=0');
text(.75, 0,'n-side');
set(gca,'DefaultTextUnits','data')
hold off
```

5.2.5 Linearly Graded Junctions

The linearly graded profile, as noted in the preliminary discussion, is a more realistic approximation for junctions formed by deep diffusions into moderate to heavily doped wafers. Redrawn in Fig. 5.13(a), the linearly graded profile is mathematically modeled by

$$N_D - N_A = ax \tag{5.40}$$

where a has units of cm^{-4} and is called the *grading constant.*

Since we seek a quantitative solution for the electrostatic variables associated with the linearly graded profile, this subsection might be viewed as an unnumbered exercise—an illustration of how the procedures established in the step junction analysis are applied to another profile. However, there are features of the linearly graded analysis that are sufficiently different to merit special consideration. First and foremost, the Eq. (5.40) profile is continuous through $x = 0$. This actually simplifies the mathematical development. It is not necessary to treat the p- and n-sides of the depletion region separately or to match the solutions at $x = 0$. There is only one ρ, $\mathscr{E}$, and V solution for the entire depletion region. Moreover, because the profile is symmetrical about $x = 0$, all of the electrostatic variables likewise exhibit a symmetry about $x = 0$. A somewhat complicating feature is the nonuniform doping *outside* of the depletion region. From previous work we know the nonuniform doping means there is a residual ρ, electric field, and potential drop external to the central depletion region. We ignore this fact, taking $\rho = 0$, $\mathscr{E} = 0$, and $V =$ constant outside of the depletion region in the development to be presented. Finally, although V is taken to be a constant outside of the depletion region, a modification of the Eq. (5.10) expression for V_{bi} is still necessary and will be included at the end of the analysis.

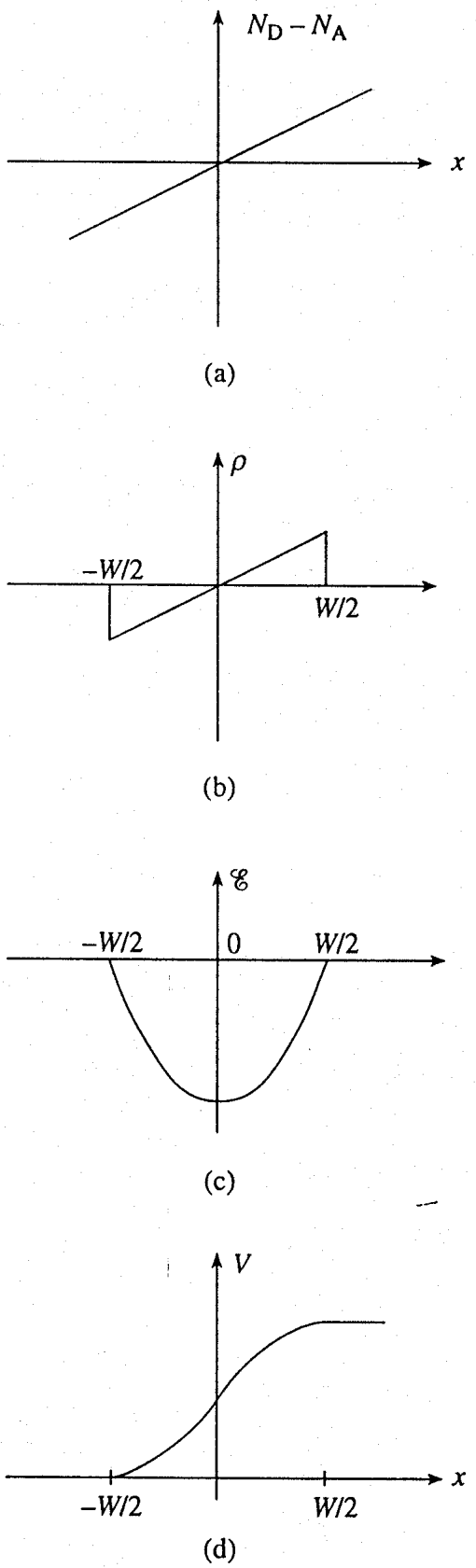

Figure 5.13 Linearly graded solution. Depletion-approximation-based quantitative solution for the electrostatic variables in a linearly graded junction. (a) Linearly graded profile. (b) Charge density, (c) electric field, and (d) electrostatic potential as a function of position.

Launching into the analysis proper by invoking the depletion approximation yields

$$\rho(x) = \begin{cases} qax & \ldots -W/2 \leq x \leq W/2 \quad (5.41a) \\ 0 & \ldots x \leq -W/2 \quad \text{and} \quad x \geq W/2 \quad (5.41b) \end{cases}$$

Note from Fig. 5.13(b) that the charge density is symmetrical about $x = 0$, and one must have

$$x_p = x_n = \frac{W}{2} \tag{5.42}$$

Substituting into Poisson's equation, separating variables, and integrating from the p-edge of the depletion region where $\mathscr{E} = 0$ to an arbitrary point x inside the depletion region then gives

$$\mathscr{E}(x) = \frac{qa}{2K_S\varepsilon_0}\left[x^2 - \left(\frac{W}{2}\right)^2\right] \qquad \ldots -\frac{W}{2} \leq x \leq \frac{W}{2} \tag{5.43}$$

A linear ρ versus x dependence naturally gives rise to a quadratic $\mathscr{E}$ versus x dependence.

Next setting $\mathscr{E}(x) = -dV/dx$, separating variables, and integrating once again from the p-edge of the depletion region where $V = 0$ to an arbitrary point x, one obtains the cubic relationship

$$V(x) = \frac{qa}{6K_S\varepsilon_0}\left[2\left(\frac{W}{2}\right)^3 + 3\left(\frac{W}{2}\right)^2 x - x^3\right] \qquad \ldots -\frac{W}{2} \leq x \leq \frac{W}{2} \tag{5.44}$$

To complete the solution, to determine W, we note that the voltage drop across the depletion region must be equal to $V_{bi} - V_A$, or $V(x) = V_{bi} - V_A$ at $x = W/2$. Making the indicated substitutions into Eq. (5.44) and solving for W, one finds

$$\boxed{W = \left[\frac{12K_S\varepsilon_0}{qa}(V_{bi} - V_A)\right]^{1/3}} \tag{5.45}$$

For future reference it is important to note that the linearly graded depletion width varies as the cube root of $V_{bi} - V_A$, whereas the step junction depletion width varies as the square root of $V_{bi} - V_A$.

Numerical computations of the linearly graded ρ, $\mathscr{E}$, and V versus x would of course require an expression for V_{bi}. The Eq. (5.10) expression for V_{bi} cannot be used because it was specifically established assuming a step junction. However, the V_{bi} derivation up to and including Eq. (5.8) places no restrictions on the doping profile other than requiring that the

doping be nondegenerate. Consequently, for nonstep junctions one merely needs to re-evaluate $n(x_n)$ and $n(-x_p)$, the electron concentrations at the edges of the equilibrium depletion region. For a linearly graded junction

$$n(x_n)_{\text{equilibrium}} \cong (N_D - N_A)|_{W_0/2} = aW_0/2 \tag{5.46a}$$

$$n(-x_p)_{\text{equilibrium}} = \frac{n_i^2}{p(-x_p)_{\text{equilibrium}}} \cong \frac{n_i^2}{-(N_D - N_A)|_{-W_0/2}} = \frac{n_i^2}{aW_0/2} \tag{5.46b}$$

where $W_0 \equiv W|_{V_A=0}$. Substituting Eqs. (5.46) into Eq. (5.8) then gives

$$V_{bi} = \frac{kT}{q} \ln\left(\frac{aW_0}{2n_i}\right)^2 = \frac{2kT}{q} \ln\left(\frac{aW_0}{2n_i}\right) \tag{5.47}$$

or, making use of Eq. (5.45),

$$V_{bi} = \frac{2kT}{q} \ln\left[\frac{a}{2n_i}\left(\frac{12K_S\varepsilon_0}{qa} V_{bi}\right)^{1/3}\right] \tag{5.48}$$

Equation (5.48) cannot be solved explicitly for V_{bi} but must be numerically iterated to determine V_{bi} for a given grading constant.

5.3 SUMMARY

The *pn* junction electrostatics covered in this chapter provides a foundation for the operational modeling of the *pn* junction diode and other devices that incorporate *pn* junctions. Early in the development we defined terms such as *profile* and *metallurgical boundary,* introduced the idealized step junction and linearly graded junction profiles used extensively in analyses, and referenced Poisson's equation, which often constitutes the starting point in obtaining quantitative solutions for the electrostatic variables. Other preliminary considerations included a qualitative solution for the electrostatic variables based on energy band arguments and the derivation of computational relationships for the built-in voltage. The depletion approximation, the most important and widely encountered of the simplifying approximations used in the modeling of devices, was introduced and illustrated.

The established formalism was initially applied to obtain quantitative solutions for the charge density, electric field, and electrostatic potential inside a step junction under equilibrium ($V_A = 0$) conditions. The analysis was subsequently extended to $V_A \neq 0$. The effect of an applied bias on the electrostatic variables was carefully examined and used to deduce the energy band diagrams for *pn* junctions under forward and reverse biasing. Finally, quantitative solutions were obtained for the electrostatic variables inside a linearly graded *pn* junction.

It is hoped the reader has acquired a qualitative feel for the electrostatic situation inside

a *pn* junction. Moreover, with the information provided, the reader, if desired, should be able to obtain quantitative solutions for the electrostatic variables associated with other doping profiles.

PROBLEMS

CHAPTER 5 PROBLEM INFORMATION TABLE				
Problem	*Complete After*	*Difficulty Level*	*Suggested Point Weighting*	*Short Description*
5.1	5.2.5	1	10 (1 each part)	True-or-false quiz
5.2	5.1.4	1	5 (a-2, b-3)	V_{bi} from energy band
5.3	5.1.4	2	13 (a-2, b-3, c-3, d-2, e-3)	Isotype step junction
5.4	5.2.2	2	12 (a-2, b-3, c-2, d-2, e-3)	Step jct. compute, $N_A \sim N_D$
5.5	5.2.2	2	12 (a-2, b-3, c-2, d-2, e-3)	Step jct. compute, $N_A \gg N_D$
• 5.6	5.2.3	2	9 (a-2, b-3, c-2, d-2)	Compute using `diary`
• 5.7	5.2.4	3	25 (a-15, b-5, c-5)	Step junction program
5.8	5.2.5	2	9 (3 each sketch)	Combination profile
5.9	"	2	9 (a-2, b-2, c-5)	Exponential profile
5.10	"	2–3	10 (a-3, b-2, c-5)	Modified-step profile
5.11	"	3–4	18 (a-8, b-2, c-8)	PIN diode
5.12	"	2–3	12 (4 each part)	Given V, find $\mathscr{E}$, ρ, $N_D - N_A$
• 5.13	"	3–4	25 (a-15, b-5, c-5)	Linearly graded program
• 5.14	"	5	35 (a-30, b-5)	Exact solution

5.1 True or false:

(a) The step junction is an idealized doping profile used to model p^+-n and n^+-p junctions.

(b) The ρ that appears in Poisson's equation is the charge density and has units of couls/cm^3.

(c) The space charge region about the metallurgical junction is due to a pile-up of electrons on the p-side and holes on the n-side.

(d) The built-in potential is typically less than the band gap energy converted to volts.

(e) Invoking the depletion approximation makes the charge density inside the depletion region directly proportional to the net doping concentration.

(f) Ohmic contacts reduce the built-in voltage drop across a junction.

(g) In solutions based on the depletion approximation, the magnitude of the electric field reaches a maximum right at the metallurgical boundary.

(h) If one has a p^+-n step junction, a junction where $N_A(p\text{-side}) \gg N_D(n\text{-side})$, then it follows that $x_p \ll x_n$.

(i) The potential hill between the n-side and the p-side of a junction increases with forward biasing.

(j) The depletion width in a linearly graded junction varies as $(V_{bi} - V_A)^{1/3}$.

5.2 A silicon step junction maintained at room temperature is doped such that $E_F = E_v - 2kT$ on the p-side and $E_F = E_c - E_G/4$ on the n-side.

(a) Draw the equilibrium energy band diagram for this junction.

(b) Determine the built-in voltage (V_{bi}) giving both a symbolic and a numerical result.

5.3 Consider the $p1$–$p2$ "isotype" step junction shown in Fig. P5.3.

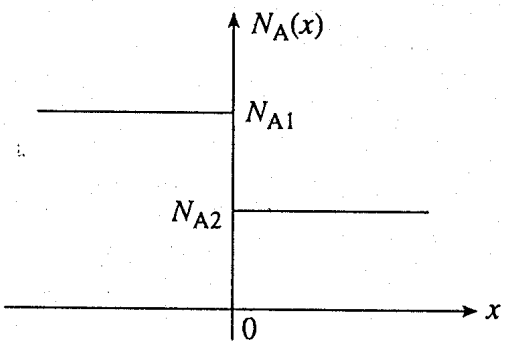

Figure P5.3

(a) Draw the equilibrium energy band diagram for the junction, taking the doping to be nondegenerate and $N_{A1} > N_{A2}$.

(b) Derive an expression for the built-in voltage (V_{bi}) that exists across the junction under equilibrium conditions.

(c) Make rough sketches of the potential, electric field, and charge density inside the junction.

(d) Briefly describe the depletion approximation.

(e) Can the depletion approximation be invoked in solving for the electrostatic variables inside the pictured $p1$–$p2$ junction? Explain.

5.4 A Si step junction maintained at room temperature under equilibrium conditions has a p-side doping of $N_A = 2 \times 10^{15}/\text{cm}^3$ and an n-side doping of $N_D = 10^{15}/\text{cm}^3$. Compute

(a) V_{bi}.

(b) x_p, x_n, and W.

(c) $\mathscr{E}$ at $x = 0$.

(d) V at $x = 0$.

(e) Make sketches that are roughly to scale of the charge density, electric field, and electrostatic potential as a function of position.

5.5 Repeat Problem 5.4, taking $N_A = 10^{17}/\text{cm}^3$ to be the p-side doping. Briefly compare the results here with those of Problem 5.4.

• **5.6** A Si step junction maintained at room temperature has a p-side doping of $N_A =$ (instructor-supplied value) and an n-side doping of $N_D =$ (instructor-supplied value). The applied voltage $V_A =$ (instructor-supplied value). Working in the *Command* window and making use of the MATLAB `diary` function to record your work session, compute

(a) V_{bi}.

(b) x_p, x_n, and W.

(c) $\mathscr{E}$ at $x = 0$.

(d) V at $x = 0$.

• **5.7** Given a nondegenerately doped silicon *pn* step junction maintained at $T = 300$ K:

(a) Compute and present coordinated plots of the electric field ($\mathscr{E}$) and electrostatic potential (V) inside the junction as a function of position (x). Assume $N_A = 10^{15}/\text{cm}^3$, $N_D = 2 \times 10^{14}/\text{cm}^3$, and $V_A = -20$ V in performing a sample computation.

Suggestions

(i) Employ the MATLAB function `subplot` to achieve coordinated plots of the electric field and electrostatic potential.

(ii) Use $(\mathscr{E}_{min}, 0)$ and $(0, V_{max})$, where $\mathscr{E}_{min} = 1.1\mathscr{E}|_{x=0}$ and $V_{max} = 1.1(V_{bi} - V_A)$, as the endpoint y-values of the electric field and potential plots, respectively. Also, with $x_{max} \equiv 2.5\text{max}(x_n, x_p)$, `max` a MATLAB function, use $(-x_{max}, x_{max})$ as the x-coordinate limits.

(b) Modify the part (a) program so that results corresponding to multiple V_A values, say $V_A = V_{A0}/2^n$ with n = 0 to 3, are simultaneously displayed. Make a printout of your results.

(c) Modify the part (b) program so that, in addition to the plots, one obtains an output list of relevant parameters and computational constants. The list is to include the following quantities: N_A, N_D, V_A, V_{bi}, x_n, x_p, W, $\mathscr{E}$ at $x = 0$, and V at $x = 0$. Print out a sample set of results.

(d) Use your program to examine how $\mathscr{E}$ versus x and V versus x vary with the relative magnitude of the doping on the two sides of the junction. Experiment, for example, with the following combinations of (N_A, N_D): $(10^{17}/\text{cm}^3, 10^{15}/\text{cm}^3)$, $(10^{16}/\text{cm}^3, 10^{15}/$

cm^3), ($10^{15}/cm^3$, $10^{15}/cm^3$), ($10^{15}/cm^3$, $10^{16}/cm^3$), ($10^{15}/cm^3$, $10^{17}/cm^3$), ($10^{18}/cm^3$, $10^{16}/cm^3$), and ($10^{16}/cm^3$, $10^{14}/cm^3$). How would you describe the results when either $N_A \geq 100N_D$ or $N_D \geq 100N_A$?

(e) Use your program to generate answers to Problems 5.4 and 5.5. Check your computer-generated results against those obtained manually.

5.8 The doping around the metallurgical junction of a special diode is pictured in Fig. P5.8. Sketch the expected charge density, electric field, and electrostatic potential inside the diode based on the depletion approximation. Properly scale and label relevant lengths. Include a few words of explanation as necessary to forestall a misinterpretation of your sketches.

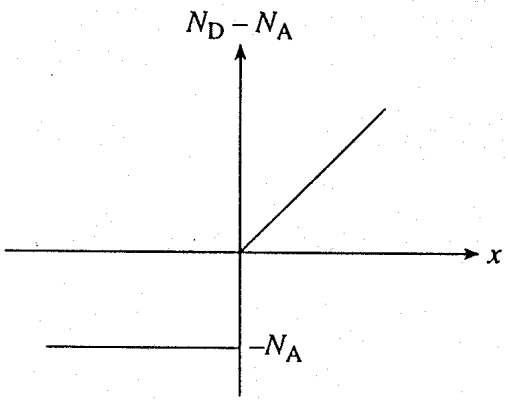

Figure P5.8

5.9 A *pn* junction diode has the doping profile sketched in Fig. P5.9. Mathematically, $N_D - N_A = N_0[1 - \exp(-\alpha x)]$, where N_0 and α are constants.

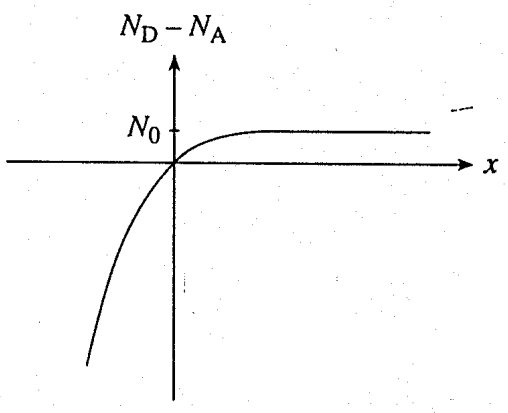

Figure P5.9

(a) Give a concise statement of the depletion approximation.

(b) Invoking the depletion approximation, make a sketch of the charge density inside the diode.

(c) Establish an expression for the electric field, $\mathscr{E}(x)$, inside the depletion region.

NOTE: The interested reader may wish to complete the electrostatic solution by obtaining expressions or computational relationships for $V(x)$, x_p, x_n, and V_{bi}. Be forewarned, however, that a considerable amount of mathematical manipulation is involved.

5.10 A *pn* junction diode has the doping profile sketched in Fig. P5.10. Make the assumption that $x_n > x_0$ for all applied biases of interest.

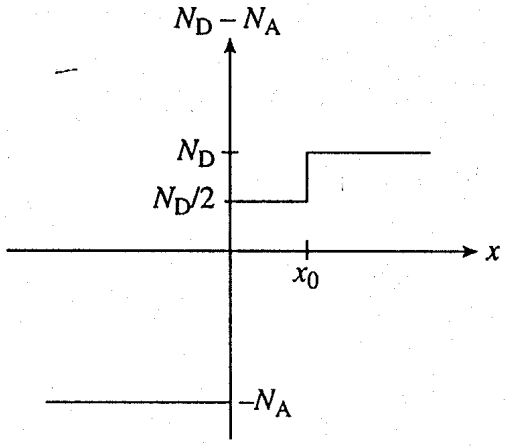

Figure P5.10

(a) What is the built-in voltage across the junction? Justify your answer.

(b) Invoking the depletion approximation, sketch the charge density ρ versus x inside the diode.

(c) Obtain an analytical solution for the electric field, $\mathscr{E}(x)$, inside the depletion region.

5.11 The *p-i-n* diode shown schematically in Fig. P5.11 is a three-region device with a middle region that is intrinsic (actually lightly doped) and relatively narrow. Assuming the *p*- and *n*-regions to be uniformly doped and $N_D - N_A = 0$ in the *i*-region:

(a) Roughly sketch the expected charge density, electric field, and electrostatic potential inside the device. Also draw the energy band diagram for the device under equilibrium conditions.

(b) What is the built-in voltage drop between the *p*- and *n*-regions? Justify your answer.

(c) Establish quantitative relationships for the charge density, electric field, electrostatic potential, and the *p*- and *n*-region depletion widths.

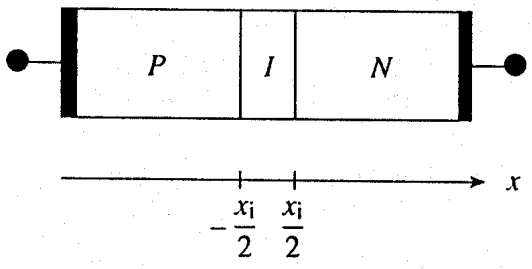

Figure P5.11

5.12 The electrostatic potential in the depletion region of a *pn* junction diode under equilibrium conditions is determined to be

$$V(x) = \frac{V_{bi}}{2}\left[1 + \sin\left(\frac{\pi x}{W}\right)\right] \quad \ldots -W/2 \leq x \leq W/2$$

(a) Establish an expression for the electric field as a function of position in the depletion region ($-W/2 \leq x \leq W/2$) and sketch $\mathscr{E}(x)$ versus x.

(b) Establish an expression for the charge density as a function of position in the depletion region and sketch $\rho(x)$ versus x.

(c) Invoking the depletion approximation, determine and sketch $N_D - N_A$ versus x in the depletion region.

• **5.13** Given a nondegenerately doped silicon *linearly graded* junction maintained at $T = 300$ K:

(a) Compute and present coordinated plots of the electric field ($\mathscr{E}$) and electrostatic potential (V) inside the junction as a function of position (x). Employ a dopant gradient constant of $a = 10^{20}/\text{cm}^4$ and an applied voltage $V_A = -20$ V in performing a sample computation. Note that Eq. (5.48) must be iterated to determine V_{bi} for a given grading constant.

(b) Modify the part (a) program so that results corresponding to multiple V_A values, say $V_A = V_{A0}/2^n$ with n = 0 to 3, are simultaneously displayed. Make a printout of your results.

(c) Change the part (b) program so that in addition to the plots one obtains an output list of relevant parameters and computational constants. The list is to include the following quantities: a, V_A, V_{bi}, W, $\mathscr{E}$ at $x = 0$, and V at $x = 0$. Print out a sample set of results.

(d) Use your program to examine how $\mathscr{E}$ versus x and V versus x vary with gradient constants over the range $10^{18}/\text{cm}^4 \leq a \leq 10^{23}/\text{cm}^4$.

(e) Compare the results obtained in this problem with the corresponding step junction results obtained in Problem 5.7.

● **5.14** If *equilibrium* conditions prevail, it is possible to obtain a closed-form solution for the electrostatic variables inside a *pn* step junction without invoking the depletion approximation. The "exact" solution valid under equilibrium ($V_A = 0$) conditions is detailed as follows:

p-side ($x \leq 0$) solution . . .

$$\int_{U_0}^{U} \frac{dU'}{F(U', U_{FP})} = \frac{x}{L_D}$$

$$\mathscr{E} = -\frac{kT}{q}\frac{1}{L_D}F(U, U_{FP})$$

$$\rho = qn_i(e^{U_{FP}-U} - e^{U-U_{FP}} + e^{-U_{FP}} - e^{U_{FP}})$$

n-side ($x \geq 0$) solution . . .

$$\int_{U_0}^{U} \frac{dU'}{F(U' - U_{BI}, U_{FN})} = \frac{x}{L_D}$$

$$\mathscr{E} = -\frac{kT}{q}\frac{1}{L_D}F(U - U_{BI}, U_{FN})$$

$$\rho = qn_i(e^{U_{FN}-U+U_{BI}} - e^{U-U_{BI}-U_{FN}} + e^{-U_{FN}} - e^{U_{FN}})$$

where . . .

$$L_D = \left[\frac{K_S \varepsilon_0 kT}{2q^2 n_i}\right]^{1/2}$$

$$F(UI, U2) = [e^{U2}(e^{-UI} + UI - 1) + e^{-U2}(e^{UI} - UI - 1)]^{1/2} \quad \text{...“}F\text{”-function}$$

$U_{FP} = \ln(N_A/n_i)$ . . . N_A is the *p*-side doping concentration

$U_{FN} = -\ln(N_D/n_i)$ . . . N_D is the *n*-side doping concentration

$$U_{BI} = U_{FP} - U_{FN} = \frac{V_{bi}}{kT/q}$$

$$U = \frac{V}{kT/q}$$

U_0 is the normalized potential (U) at $x = 0$. The value of U_0 is obtained by solving the transcendental equation: $F(U_0, U_{FP}) = F(U_0 - U_{BI}, U_{FN})$. This relationship results from the fact that the electric field must be continuous at $x = 0$.

(a) Using the preceding relationships, construct coordinated plots of the electric field ($\mathscr{E}$) and the electrostatic potential, $V = (kT/q)U$, inside the *pn* junction as a function of position. Assume $N_A = 10^{15}/\text{cm}^3$ and $N_D = 2 \times 10^{14}/\text{cm}^3$ in performing a sample computation. If available, also run the Problem 5.7(a) program utilizing an identical set of parameters. Compare and discuss the two sets of $\mathscr{E}$, V versus x plots.

Suggestions

(i) First determine U_0 employing the MATLAB function `fzero` with an initial guess of $U_0 = U_{BI}/2$.

(ii) Stepping U from 0.1 to U_0 and utilizing the integral relationship, compute $U = V/(kT/q)$ versus x on the p-side of the junction. Repeat for the n-side, stepping U from U_0 to $U_{BI} - 0.1$.

(iii) For each value of U in step (ii), likewise compute $\mathscr{E}$. Knowing $\mathscr{E}$ versus U and U versus x allows one to construct an $\mathscr{E}$ versus x plot.

(iv) In constructing the $\mathscr{E}$ and V plots, follow the suggestions cited in Problem 5.7(a).

(b) Extend the part (a) computations to obtain the normalized charge density (ρ/q) versus x. On a single set of coordinates, construct a sample plot of ρ/q versus x as deduced from both the exact and depletion-approximation-based solutions. Discuss your plotted results.